Department of Physics
Institute for Theoretical Physics
University of Tübingen, Germany
Master Degree in Astro & Particle Physics
Academic Year 2024-2025
October 31, 2025

Master's Thesis

Transverse Spin Effects at NLO Accuracy in Semi-Inclusive Deep Inelastic Scattering

---

Supervisor:
Prof. Marc Schlegel

Student:
Diego Scantamburlo

Co-supervisor:
Prof. Werner Vogelsang

…

Contents

Introduction

Lorem ipsum dolor sit amet, consectetuer adipiscing elit. Ut purus elit, vestibulum ut, placerat ac, adipiscing vitae, felis. Curabitur dictum gravida mauris. Nam arcu libero, nonummy eget, consectetuer id, vulputate a, magna. Donec vehicula augue eu neque. Pellentesque habitant morbi tristique senectus et netus et malesuada fames ac turpis egestas. Mauris ut leo. Cras viverra metus rhoncus sem. Nulla et lectus vestibulum urna fringilla ultrices. Phasellus eu tellus sit amet tortor gravida placerat. Integer sapien est, iaculis in, pretium quis, viverra ac, nunc. Praesent eget sem vel leo ultrices bibendum. Aenean faucibus. Morbi dolor nulla, malesuada eu, pulvinar at, mollis ac, nulla. Curabitur auctor semper nulla. Donec varius orci eget risus. Duis nibh mi, congue eu, accumsan eleifend, sagittis quis, diam. Duis eget orci sit amet orci dignissim rutrum.

Nam dui ligula, fringilla a, euismod sodales, sollicitudin vel, wisi. Morbi auctor lorem non justo. Nam lacus libero, pretium at, lobortis vitae, ultricies et, tellus. Donec aliquet, tortor sed accumsan bibendum, erat ligula aliquet magna, vitae ornare odio metus a mi. Morbi ac orci et nisl hendrerit mollis. Suspendisse ut massa. Cras nec ante. Pellentesque a nulla. Cum sociis natoque penatibus et magnis dis parturient montes, nascetur ridiculus mus. Aliquam tincidunt urna. Nulla ullamcorper vestibulum turpis. Pellentesque cursus luctus mauris.

Nulla malesuada porttitor diam. Donec felis erat, congue non, volutpat at, tincidunt tristique, libero. Vivamus viverra fermentum felis. Donec nonummy pellentesque ante. Phasellus adipiscing semper elit. Proin fermentum massa ac quam. Sed diam turpis, molestie vitae, placerat a, molestie nec, leo. Maecenas lacinia. Nam ipsum ligula, eleifend at, accumsan nec, suscipit a, ipsum. Morbi blandit ligula feugiat magna. Nunc eleifend consequat lorem. Sed lacinia nulla vitae enim. Pellentesque tincidunt purus vel

magna. Integer non enim. Praesent euismod nunc eu purus. Donec bibendum quam in tellus. Nullam cursus pulvinar lectus. Donec et mi. Nam vulputate metus eu enim. Vestibulum pellentesque felis eu massa.

Quisque ullamcorper placerat ipsum. Cras nibh. Morbi vel justo vitae lacus tincidunt ultrices. Lorem ipsum dolor sit amet, consectetuer adipiscing elit. In hac habitasse platea dictumst. Integer tempus convallis augue. Etiam facilisis. Nunc elementum fermentum wisi. Aenean placerat. Ut imperdiet, enim sed gravida sollicitudin, felis odio placerat quam, ac pulvinar elit purus eget enim. Nunc vitae tortor. Proin tempus nibh sit amet nisl. Vivamus quis tortor vitae risus porta vehicula.

Fusce mauris. Vestibulum luctus nibh at lectus. Sed bibendum, nulla a faucibus semper, leo velit ultricies tellus, ac venenatis arcu wisi vel nisl. Vestibulum diam. Aliquam pellentesque, augue quis sagittis posuere, turpis lacus congue quam, in hendrerit risus eros eget felis. Maecenas eget erat in sapien mattis porttitor. Vestibulum porttitor. Nulla facilisi. Sed a turpis eu lacus commodo facilisis. Morbi fringilla, wisi in dignissim interdum, justo lectus sagittis dui, et vehicula libero dui cursus dui. Mauris tempor ligula sed lacus. Duis cursus enim ut augue. Cras ac magna. Cras nulla. Nulla egestas. Curabitur a leo. Quisque egestas wisi eget nunc. Nam feugiat lacus vel est. Curabitur consectetuer.

Suspendisse vel felis. Ut lorem lorem, interdum eu, tincidunt sit amet, laoreet vitae, arcu. Aenean faucibus pede eu ante. Praesent enim elit, rutrum at, molestie non, nonummy vel, nisl. Ut lectus eros, malesuada sit amet, fermentum eu, sodales cursus, magna. Donec eu purus. Quisque vehicula, urna sed ultricies auctor, pede lorem egestas dui, et convallis elit erat sed nulla. Donec luctus. Curabitur et nunc. Aliquam dolor odio, commodo pretium, ultricies non, pharetra in, velit. Integer arcu est, nonummy in, fermentum faucibus, egestas vel, odio.

Chapter 1

Hadronic matrix elements at sub-leading twist

In order to obtain a factorized spin-dependent cross section for SIDIS, involving twist-3 contributions, we will need several so called *soft* matrix elements. The "nucleon-to-parton" process, as well as the "parton-to-hadron" hadronization phenomenon, are typically described through non-perturbative matrix elements of certain QCD operators. In principle, they contain all relevant information about the distribution of quarks and gluons inside the nucleon, as well as the decay process from "free" quarks and gluons into color-neutral states such as baryons and mesons. The inner hadronic structure is therefore encoded in these non-perturbative objects. Since they are non-perturbative, they cannot be computed from first principles in QCD. However, they can be extracted from experimental data [**<empty citation>**] or computed using non-perturbative methods such as lattice QCD or QCD sum rules [**<empty citation>**]. It is therefore clear that a thorough understanding of these matrix elements is essential in order to study high-energy scattering processes involving hadrons. For the study of unpolarized cross sections, the relevant matrix elements are closely related to the so called parton distribution functions (PDFs) and fragmentation functions (FFs). PDFs describe the distribution of partons inside a hadron, while FFs describe the hadronization of partons into hadrons. Both PDFs and FFs can be classified according to their twist, which is a measure of their relevance in high-energy processes. Leading-twist PDF s and FFs are the most important ones, as they dominate the cross section at

high energies. However, sub-leading twist PDFs and FFs also play a significant role in certain processes, especially when spin degrees of freedom are involved. In this chapter, we will introduce the relevant twist-3 PDFs and FFs that will be used in the following chapters to derive a factorized expression for the SIDIS cross section involving twist-3 contributions. We will also discuss some important relations among these functions that will be crucial in our analysis.

1.1 Light-cone coordinates and twist

See beginning of chap 2 + Jaffe or whatever it's called

1.2 Multi-parton correlations

ADD HERE DISTINCTION DISTRIBUTION/FRAGMENTATION

1.2.1 Leading-twist distributions

The relevant hadronic matrix element describing the "nucleon-to-quark" process is given by the so-called quark-quark distribution correlator

$$\begin{aligned}\Phi^q_{ij}(x) &= \int \frac{\mathrm{d}\lambda}{2\pi}\, e^{i\lambda x}\, \langle N(P,S)|\bar{\psi}^q_j(0)\psi^q_i(\lambda n)|N(P,S)\rangle \\ &= \frac{1}{2}\left(\not{P}\right)_{ij} f^q_1(x) - \frac{1}{4}\left(\left[\not{P},\not{S}\right]\gamma_5\right)_{ij} h^q_1(x) + \cdots .\end{aligned} \tag{1.1}$$

The different Dirac structures appearing in the correlator are parametrized by the so-called parton distribution functions (PDFs) $f_1(x)$ and $h_1(x)$, which are referred to as the leading-twist unpolarized and transversity parton densities. The former often enters the unpolarized observables, and it has been extensively determined by numerous experimental collaborations throughout the years [**<empty citation>**]. In other words,

$f_1(x)$ is arguably the most constrained and the best understood PDF among all non-perturbative functions in hadronic physics. The latter, on the other hand, is present only if the nucleon is transversely polarized. Although being a leading twist effect, transversity has been known with satisfactory accuracy only in recent years [10]. This is mainly linked to the fact that it is experimentally challenging to set up and control transversely polarized hadronic targets. This is even more true for transversely polarized beams, which is currently one of the experimental frontiers when it comes to the field of hadronic spin physics.

One may also have an equivalent hadronic matrix element describing the "nucleon-to-gluon" process, also often appearing in hadronic observables. It is described through the gluon-gluon distribution correlator CHECK

$$\begin{aligned}\Phi^{g,\mu\nu}(x) &= \int \frac{\mathrm{d}\lambda}{2\pi}\, e^{i\lambda x}\, \langle N(P,S)|CHANGE|N(P,S)\rangle \\ &= \frac{1}{2} g_T^{\mu\nu} \left(\not{P}\right)_{ij} f_1^g(x) + \cdots ,\end{aligned} \tag{1.2}$$

where $f_1^g(x)$ is the leading-twist unpolarized gluon distribution functions. Again, the gluonic contribution entering the unpolarized PDFs is also well understood. As we will see later, in semi-inclusive deep inelastic scattering this correlator only appears at next-to-leading order in the strong coupling. This is because the gluon coming from the nucleon cannot directly couple to the virtual photon, and hence an additional partonic subprocess of order $\mathcal{O}(\alpha_S)$ must occur. In any case, it is quite useful to visualize these objects in a Feynman cut diagram notation [24, 6]. In fact, if one writes down the total squared amplitude $|\mathcal{A}|^2$ for a given hadronic scattering process assuming the parton model, it is easy to realize that these soft hadronic matrix elements are indeed ubiquitous in high-energy physics. The two distribution correlators are shown in Fig. 1.1.

1.2.2 Intrinsic twist-3 fragmentation

The first type of sub-leading twist hadronic matrix elements are the so called *intrinsic* twist-3 functions. They are expressed in terms of 2-parton correlations, involving a pair of quark fields or a pair of gluons. The fact that only one parton (on each side of

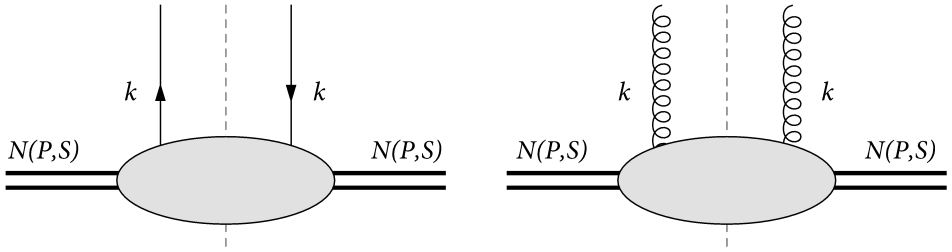

Figure 1.1: Quark-quark (left) and gluon-gluon (right) distribution correlators appearing at leading-twist.

the cut) is participating in the distribution/fragmentation process is a common feature with leading twist correlations.
Starting with the quark-quark case, these quantities are organized into a quark-quark fragmentation correlator

$$\begin{aligned}\Delta^q_{ij}(z) &= \sum_X \int \frac{\mathrm{d}\lambda}{2\pi}\, e^{-i\frac{\lambda}{z}}\, \langle 0|\psi^q_i(0)|h(P_h);X\rangle\ \langle h(P_h);X|\bar{\psi}^q_j(\lambda m)|0\rangle \\ &= \frac{1}{z}\left(\not{P}_h\right)_{ij} D^q_1(z) - \frac{iM_h}{2z}\left(\left[\not{P}_h,\not{n}\right]\right)_{ij} H^q(z) + \frac{M_h}{z}(\not{k})_{ij}\, E^q(z) + \cdots ,\end{aligned} \tag{1.3}$$

where again the dots denote terms that are irrelevant for the present analysis. The $D_1(z)$ term is the familiar twist-2 unpolarized fragmentation function, appearing in numerous different high-energy processes involving the production of unpolarized hadrons. The sub-leading twist fragmentation function $H(z)$ describes the (power suppressed) production of unpolarized hadrons in the final state. The fact that twist-3 effects are generally smaller compared to the leading-twist case can be easily spotted by the fact they come with a mass factor M_h, the hadron mass. Compared to any hard scale, which we consider to be at least of the order of a some GeV's, typical produced hadron masses range from a few hunder MeV's (π) all they way up to a few GeV's (Λ). In this sense, the effect is said to be power suppressed.
One can also build a matrix element in which the exchanged parton coming from the nucleon is not a quark but rather a gluon. In this case, we only have leading twist

effects, described in terms of a gluon-gluon fragmentation correlator CHECK

$$\begin{aligned}\Delta^{g,\mu\nu}(z) &= \sum_X \int \frac{\mathrm{d}\lambda}{2\pi}\, e^{-i\frac{\lambda}{z}} CHECK \\ &= \frac{1}{z} g_T^{\mu\nu} \left(\not{P}_h\right)_{ij} D_1^g(z) + \cdots ,\end{aligned} \tag{1.4}$$

where $D_1^g(z)$ is the unpolarized gluon fragmentation function.

Similarly to distribution matrix elements, also fragmentation correlators are conveniently depicted as cut diagrams, as shown in Fig. 1.2.

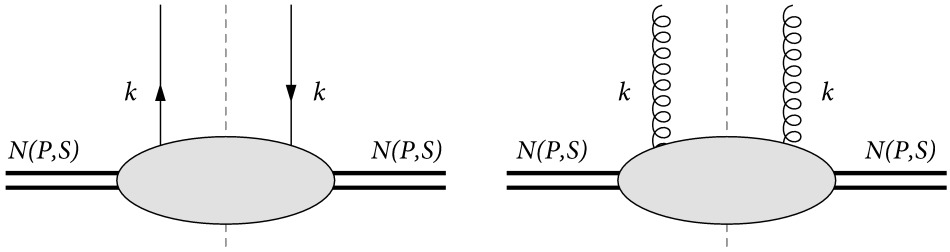

Figure 1.2: Soft matrix elements relevant for leading twist and intrinsic twist-3 fragmentation. The quark-quark correlator (left) can depict both $D_1(z)$ or $H(z)$ depending on the Dirac structure assumed. The gluon-gluon correlator is also shown (right).

1.2.3 Kinematical twist-3 fragmentation

Another kind of two-parton correlation functions are the so called *kinematical* twist-3 functions. Contrary to the intrinsic twist-3 case, these objects incorporate (indirectly) also the transverse momentum dependence of partons. Instead of assuming the hadron and the fragmenting parton to be exactly collinear, now the kinematical approximation to the partonic momentum reads

$$p^\mu = \frac{1}{z} P_h^\mu + p_T^\mu, \tag{1.5}$$

where p_T denotes the transverse partonic momentum. In practice, one performs a Taylor expansion to first order in p_T in the hard scattering subprocess, commonly called

the *collinear expansion*. After this expansion, one often integrates out the transverse momentum, leaving us with a collinear matrix element. Keeping at first the full p_T-dependence into account, one may define a transverse momentum dependent (TMD) fragmentation correlator

$$\begin{aligned}\Delta^q_{ij}(z,p_T) &= \sum_X \int \frac{\mathrm{d}\lambda}{2\pi} \int \frac{\mathrm{d}^{d-2}\eta_T}{(2\pi)^2}\, e^{-i\frac{\lambda}{z}-i\eta_T\cdot p_T} \\ &\qquad \times \langle 0|\psi^q_i(0)|h(P_h);X\rangle\ \langle h(P_h);X|\bar\psi^q_j(\lambda m+\eta_T)|0\rangle \\ &= \frac{izM_h}{2}\big[\not P_h,\not\eta\big]H^q(z,p_T) + \frac{iz}{2M_h}\big[\not p_T,\not P_h\big]H_1^{\perp,q}(z,p_T) \\ &\quad + zM_h(\not\epsilon)_{ij}\,E^q(z,p_T)+\cdots\,.\end{aligned} \tag{1.6}$$

COMMENT ON FUNCTIONS
Now, the collinear matrix element relevant within the collinear twist-3 formalism is nothing else but the p_T-weighted correlator. It is

$$\begin{aligned}\Delta^\rho_{\partial,ij}(z) &= \int \mathrm{d}^{d-2}p_T\, p_T^\rho\, \Delta_{ij}(z,p_T) \\ &= \frac{z^{2\epsilon}}{z}\frac{iM_h}{2}\left(\big[\not P_h,\gamma^\rho\big] - \big[\not P_h,\not\eta\big]P_h^\rho\right)_{ij} H_1^{\perp(1)}(z)+\cdots\,,\end{aligned} \tag{1.7}$$

where the first moment of the Collins function is defined as the first $\vec{p_T}$ moment of the TMD fragmentation function CHECK Z!

$$H_1^{\perp(1)}(z) = z^2\int \mathrm{d}^2p_T \frac{\vec{p_T}^{\,2}}{2M_h^2} H_1^\perp(z,z^2p_T^2). \tag{1.8}$$

Kinematical twist-3 matrix elements are pictorially represented by the same kind of diagrams as the intrinsic twist-3 case. However, the kinematical approximation is different and one should keep in mind that the partonic momentum should have a transverse component, as shown in Fig. 1.3

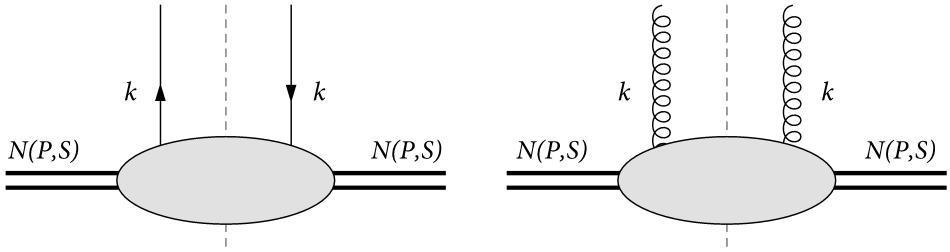

Figure 1.3: Soft matrix element relevant for kinematical twist-3 fragmentation.

1.2.4 Dynamical twist-3 fragmentation

The last type of twist-3 correlators are described in terms of matrix elements of three partonic fields, typically two quark/anti-quark fields and one gluonic field strength tensor. In general, such structures are composed of an interference of two transition amplitudes: one that is a coherent fragmentation of two partons into a hadron, and another that is the ordinary one-parton fragmentation. These objects are usually called *dynamical* twist-3 correlation functions. Since the partons contributing to the hadron production are two, it makes sense that the matrix element will depend on more than one momentum fraction. The partonic momenta are now approximated as

$$p^\mu = \frac{1}{z} P_h^\mu, \qquad p'^\mu = \frac{1}{z'} P_h^\mu. \tag{1.9}$$

It is customary to introduce a scaled variable for the z' momentum fraction, $z' = z/\zeta$, since it will simplify the treatment later on.

One type of dynamical twist-3 matrix elements are the so called *quark-gluon-quark correlations*. In this case a quark and a gluon contribute to the final state hadronization process. The correlator is written as

$$\begin{aligned}\Delta^{qg,\rho}_{F,ij}(z,\zeta) = \sum_X \int \frac{\mathrm{d}\lambda}{2\pi} \int \frac{\mathrm{d}\eta}{2\pi}\, e^{-i\frac{\lambda}{z}\zeta - i\frac{\eta}{z}(1-\zeta)}\, \langle 0|ig_S\mu^\epsilon m_\sigma F^{\sigma\rho}(\eta m)\psi_i(0)|h(P_h);X\rangle \\ \times\, \langle h(P_h);X|\bar{\psi}_j(\lambda m)|0\rangle \\ = z^{2\epsilon}\frac{iM_h}{2z}\left(\left[\not{P}_h,\gamma^\rho\right] - \left[\not{P}_h,\not{\eta}\right]P_h^\rho\right)_{ij}\, i\left(\hat{H}^{qg}_{FU}(z,z')\right)^* + \cdots,\end{aligned} \tag{1.10}$$

where $\hat{H}^{qg}_{FU}$ is the quark-gluon-quark fragmentation function describing the production

of unpolarized hadrons.

Another kind of dynamical twist-3 matrix element is given by a quark-antiquark-gluon correlation. Intuitively, the fragmentation is initiated from a quark-antiquark pair. The relevant correlator is CHECK

$$\begin{aligned}\Delta_{F,ij}^{q\bar{q},\rho}(z,\zeta) &= \sum_X \int \frac{\mathrm{d}\lambda}{2\pi} \int \frac{\mathrm{d}\eta}{2\pi}\, e^{-i\frac{\lambda}{z}\zeta - i\frac{\eta}{z}(1-\zeta)} CHECK \\ &\qquad\qquad CHECK \\ &= z^{2\epsilon}\frac{iM_h}{2z}\left(\left[\not{P}_h,\gamma^\rho\right] - \left[\not{P}_h,\not{n}\right]P_h^\rho\right)_{ij}\, i\left(\hat{H}_{FU}^{q\bar{q}}(z,z')\right)^* + \cdots ,\end{aligned} \tag{1.11}$$

ADD HERE BOUNDARY CONDITIONS AND SYMMETRIES ETC...

Lastly, the diagram notation for these dynamical twist-3 correlations is presented in Fig. 1.4

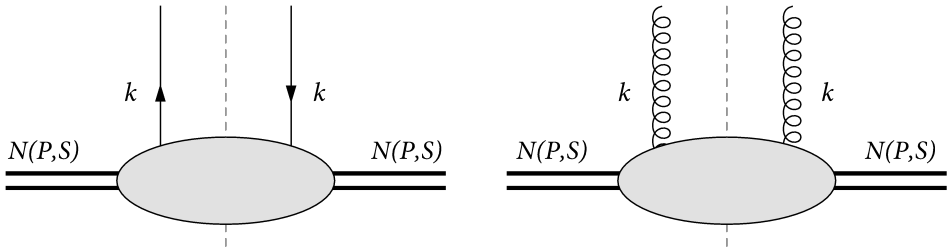

Figure 1.4: Soft matrix element relevant for dynamical twist-3 fragmentation. Quark-gluon-quark (right) and quark-antiquark-gluon (left) correlations are shown.

1.3 QCD equation of motion relations

ADD LITTLE DERIVATION OF EOM IN D DIMENSIONS! RELEVANT FOR THIS WORK!

The previously introduced twist-3 fragmentation functions are not independent from each other. In fact, they are related through the QCD equation of motion. The corresponding constraint equations will be referred as *equation of motion relations* (EoMRs). These relations between sub-leading twist matrix elements can be derived by applying the QCD EOM to the relevant quark fields appearing in the correlators. The quark fields satisfy the equation

$$\left(i\not{D}(x) - m_q\right)\psi^q(x) = 0 \tag{1.12}$$

where $D^{ab}_\mu(x) = \delta^{ab}\partial_\mu - ig_S G^{ab}_\mu(x)$ is the usual covariant derivative in the fundamental representation. Decomposing the above equation on the light-cone and considering the matrix elements appearing in the various correlators [2], one can derive the following relation [14]

$$\frac{H^a(z)}{2z} + H_1^{\perp(1)a}(z) = \mathcal{P}\int_0^1 \mathrm{d}\zeta \frac{\mathrm{Im}[\hat{H}^a_{FU}(z, z/\zeta)]}{1-\zeta} \qquad \text{(EoMR)}\,. \tag{1.13}$$

Similar relations hold also for all the other twist-3 fragmentation functions, as well as for twist-3 parton distribution functions. Since other contributions do not enter our spin-dependent SIDIS cross section in the polarization case of interest, such EoMRs are irrelevant for the present work and we omit them here for brevity. At first glance, the above relation may seem redundant since it simply expresses the intrinsic and kinematical twist-3 fragmentation functions in terms of the dynamical one. However, as we will see in the next chapters, this relation is crucial to obtain a gauge invariant and infrared (IR) safe result for the final twist-3 cross section. In fact, when computing the hard scattering coefficients, one finds that they are not separately gauge invariant. Only after combining them according to the above EoMR, one obtains a gauge invariant result. This is a strong indication that the application of the QCD EoMR is not optional but it is rather an important and essential step in this kind of calculations.

ADD HERE GLUON EOMRs???

We also note in passing that one can find yet another fragmentation function in the literature, often denoted as $\tilde{H}(z)$. This functions is nothing else but a shorthand for a particular combination of H and $H_1^{\perp(1)}$ or, equivalently, an (integrated) $\hat{H}_{FU}$ quark-

gluon-quark correlation function. It is defined as

$$\tilde{H}^a(z) = 2z\,\mathcal{P}\int_0^1 \mathrm{d}\zeta \frac{\mathrm{Im}[\hat{H}^a_{FU}(z,z/\zeta)]}{1-\zeta} = H^a(z) + 2z\,H_1^{\perp(1)a}(z). \tag{1.14}$$

It is worth mentioning that this specific fragmentation function will play an important role in Chap. 4, when some numerical explorations of the $A_{UT}^{\sin\phi_S}$ asymmetry will be performed. In fact, for the first time, this collinear quark-gluon-quark function $\tilde{H}(z)$ has been extracted only recently from experimental data [10].

1.4 Lorentz invariance relations

Interestingly, there is yet another set of relations among twist-3 fragmentation functions, which are derived from the requirement of Lorentz invariance. These relations, called *Lorentz invariance relations* (LIRs), can be obtained by considering the most general decomposition of the relevant correlators in terms of all possible Lorentz structures. By imposing that the correlators transform correctly under Lorentz transformations, one can derive constraints on the fragmentation functions and parton distribution functions. In particular, one finds that certain combinations of twist-3 fragmentation functions must vanish. For our purposes, the most relevant LIR is [14]

$$\frac{H^a(z)}{z} = -\left(1 - z\frac{\mathrm{d}}{\mathrm{d}z}\right) H_1^{\perp(1)a}(z) - 2\int_0^1 \mathrm{d}\zeta \frac{\mathrm{Im}[\hat{H}^a_{FU}(z,z/\zeta)]}{(1-\zeta)^2} \qquad (\mathrm{LIR})\,. \tag{1.15}$$

Very similarly to the EoMR case, this relation can be essential to obtain a Lorentz invariant twist-3 cross section. In fact, a priori, twist-3 cross sections may be frame dependent, since the partonic coefficients depend on the light-cone vectors n^μ and m^μ, which in turn depend on the choice of reference frame. As clearly seen in the previous paragraphs, the parametrization of twist-3 matrix elements depends explicitly on these vectors. The fact that twist-3 observables explicitly involve these light-cone vectors is intuitively clear. This is because any twist-3 observable is sensitive to the transverse component of some vector (e.g. the transverse spin component, etc...) and in order to define what "transverse" means one needs to introduce two light-cone vectors. As one sees, it is only after applying LIRs that one obtains a frame independent result and sees the manifest Lorentz invariance of the cross section.

Chapter 2

Semi-inclusive deep inelastic scattering and the A_{UT} asymmetry

2.1 Kinematics, frame and factorization

As anticipated, we study the semi-inclusive lepton-nucleon process described by

$$e(l) + N(P, S) \longrightarrow e(l') + h(P_h) + X. \tag{2.1}$$

Defining the space-like momentum of the virtual photon as $q^\mu = l^\mu - l'^\mu$, the usual SIDIS kinematical variables are given by

$$x_B = \frac{Q^2}{2P \cdot q}, \qquad y = \frac{P \cdot q}{P \cdot l}, \qquad z_h = \frac{P \cdot P_h}{P \cdot q}. \tag{2.2}$$

For reasons that will hopefully be clear soon, the initial factorization of the cross section is conveniently derived in a frame in which the nucleon and hadron momenta are collinear along the z axis. As typical in a pQCD calculation, we neglect all lepton and hadron masses, since we are interested in the high-energy scattering limit. This means that both the nucleon and the outgoing hadron momenta are approximately light-like vectors, i.e. $P^2 = P_h^2 \approx 0$. It is therefore natural to introduce transverse projectors that specify the components of any 4-vector that is transverse to both the nucleon and

the hadron momenta. The projector in this frame reads

$$g_T^{\mu\nu} = g^{\mu\nu} - \frac{1}{P \cdot P_h}(P^\mu P_h^\nu + P^\nu P_h^\mu). \tag{2.3}$$

It is also useful to introduce a set of auxiliary light-cone vectors $n^\mu = \frac{2x_B}{z_h Q^2} P_h^\mu$ with $n^2 = 0$ and $n \cdot P = 1$, along with $m^\mu = \frac{2x_B}{z_h Q^2} P^\mu$ with $m^2 = 0$ and $m \cdot P_h = 1$. The transverse projector can then be cast in the following equivalent form

$$g_T^{\mu\nu} = g^{\mu\nu} - n^\mu P^\nu - n^\nu P^\mu = g^{\mu\nu} - m^\mu P_h^\nu - m^\nu P_h^\mu. \tag{2.4}$$

With this conventions, a transverse vector will be simply denoted as $a_T^\mu = g_T^{\mu\nu} a_\nu$. In this frame, we have the following parametrization of the four-vectors $a^\mu = (a^0, \vec{a})$ [**<empty citation>**]:

$$\begin{aligned} P^\mu &= \Big(\frac{Q}{2x_B}, 0, 0, \frac{Q}{2x_B}\Big), \\ P_h^\mu &= \Big(\frac{z_h Q}{2}, 0, 0, -\frac{z_h Q}{2}\Big), \\ q^\mu &= \Big(\frac{Q_T^2}{2Q}, Q_T \cos\phi_q, Q_T \sin\phi_q, -Q + \frac{Q_T^2}{2Q}\Big), \\ q_T^\mu &= \Big(0, Q_T \cos\phi_q, Q_T \sin\phi_q, 0\Big), \end{aligned} \tag{2.5}$$

where $Q_T = \sqrt{-q_T^2}$. It is therefore clear that in a frame where the nucleon and the outgoing hadron are collinear, a light-cone decomposition is possible and the meaning of "transverse" with respect to the hadron momenta is clearly understood. The 4-dimensional space is hence partitioned in a "plus" direction, a "minus" direction and a 2-dimensional transverse space. For a generic 4-vector a^μ, the following decomposition holds

$$a^\mu = (a \cdot n)P^\mu + (a \cdot P)n^\mu + a_T^\mu = (a \cdot m)P_h^\mu + (a \cdot P_h)m^\mu + a_T^\mu. \tag{2.6}$$

By denoting as k^μ the momentum of the parton coming from the nucleon, and p^μ the fragmenting partonic momentum, we have

$$\begin{aligned} k^\mu &= xP^\mu + k_T^\mu + (k \cdot P)n^\mu \approx xP^\mu + k_T^\mu, \\ p^\mu &= \frac{1}{z}P_h^\mu + p_T^\mu + (p \cdot P_h)m^\mu \approx \frac{1}{z}P_h^\mu + p_T^\mu, \end{aligned} \tag{2.7}$$

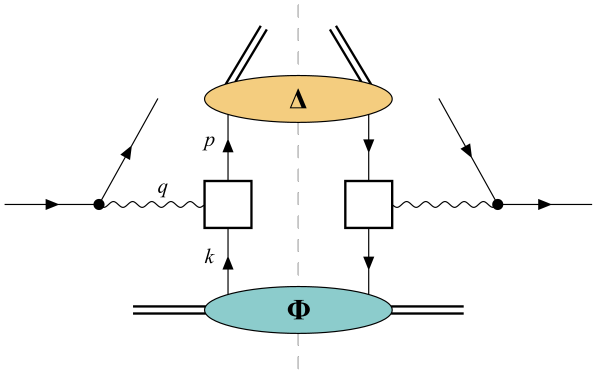

Figure 2.1: Caption

where, as typical, we neglected contributions of order two or higher in the transverse momenta. Note that this approximation is consistent with the application of the collinear twist-3 formalism, since we will need only linear terms in k_T or p_T to fully derive a factorized spin-dependent cross section.

The relevant Feynman diagrams for SIDIS at LO are given in Fig. 2.1. The lower and upper colored blobs are nothing else but non-perturbative matrix elements introduced in the previous chapter. For a direct generalization to NLO, we isolate the hard-scattering amplitude $\hat{\mathcal{M}}$ of the partonic subprocess with the virtual photon. The differential cross section is then obtained by employing QCD and QED Feynman rules and hadronic matrix elements [25]. For direct generalization to a NLO case, we perform the calculation in dimensional regularization in $d = 4 - 2\epsilon$ dimensions. We obtain

$$\mathrm{d}\sigma = \frac{1}{F} \frac{\mathrm{d}^{d-1}\boldsymbol{l}'}{(2\pi)^{d-1} 2E'} \frac{\mathrm{d}^{d-1}\boldsymbol{P_h}}{(2\pi)^{d-1} 2E_h} \frac{(4\pi)^2 \alpha_{em}^2}{Q^4} L^{\mu\nu} W_{\mu\nu}, \tag{2.8}$$

with the leptonic tensor $L^{\mu\nu}$ defined as

$$L^{\mu\nu} = \frac{1}{2} \mathrm{Tr}\Big[(1 + \lambda_e \gamma_5) \not{l} \gamma^\nu \not{l}' \gamma^\mu\Big], \tag{2.9}$$

where λ_e denotes the helicity of the incoming lepton. The hadronic tensor $W_{\mu\nu}$, evi-

dently, assumes different forms depending on the reaction channel. We derive

$$\begin{aligned}
W_{\mu\nu}^{q\to q} &= \sum_a e_a^2 \int \mathrm{d}^d k \int \mathrm{d}^d p\, \delta^{(d)}(q+k-p)\, \mathrm{Tr}\Big[\hat{\mathcal{M}}_\mu^{q\to q}\Phi^a \hat{\bar{\mathcal{M}}}_\nu^{q\to q}\Delta^a\Big] \\
W_{\mu\nu}^{gq\to q} &= \sum_a e_a^2 \int \mathrm{d}^d k \int \mathrm{d}^d p \int \mathrm{d}^d k'\, \delta^{(d)}(q+k-p)\, \mathrm{Tr}\left[\frac{\hat{\mathcal{M}}_{\mu\sigma}^{gq\to q}}{g_S T^\alpha}\Phi_A^{\sigma,a} \hat{\bar{\mathcal{M}}}_\nu^{q\to q}\Delta^a\right] \\
W_{\mu\nu}^{q\to gq} &= \sum_a e_a^2 \int \mathrm{d}^d k \int \mathrm{d}^d p \int \mathrm{d}^d p'\, \delta^{(d)}(q+k-p)\, \mathrm{Tr}\left[\frac{\hat{\mathcal{M}}_{\mu\sigma}^{q\to gq}}{g_S T^\alpha}\Phi^a \hat{\bar{\mathcal{M}}}_\nu^{q\to q}\Delta_A^{\sigma,a}\right]
\end{aligned} \tag{2.10}$$

with $\Phi^a, \Delta^a, \Phi_A^{\sigma,a}\Delta_A^{\sigma,a}$ the correlators introduced in the previous chapter, but in their fully-unintegrated versions. Here, the $\sum_a$ really just means a sum over quarks and anti-quarks flavours ($a = q, \bar{q}$). All momenta are now decomposed through the light-cone decomposition introduced before. Performing the (trivial) integrations over $\mathrm{d}(k\cdot P)$ and $\mathrm{d}(p\cdot P_h)$, one sees that the integral measures and the delta function arrange in the following way

$$\begin{aligned}
\mathrm{d}^d k\, \mathrm{d}^d p\, \delta^{(d)}(q+k-p) \sim{}& \mathrm{d}x\, \mathrm{d}^{d-2}k_T\, \frac{\mathrm{d}z}{z^2}\, \mathrm{d}^{d-2}p_T \\
&\times \frac{2x_B z_h}{Q^2}\delta(x - x_B(1-\chi_T^2))\delta(z-z_h)\delta^{(d-2)}(\vec{q}_T + \vec{k}_T - \vec{p}_T).
\end{aligned} \tag{2.11}$$

We stress that the separation of the delta function in such a way makes sense only in a frame where the nucleon and the hadron are collinear, i.e. the PP_h frame used so far. In this case, the transverse vectors are indeed 2-dimensional and this kind of $(+,-,T)$ separation makes sense.

Our goal is to study the differential cross section integrated over transverse momentum of the observed hadron. However, in a collinear frame such as the one used so far, the momentum P_h is fixed and it has no transverse component by construction. A possible approach would be to integrate over the transverse momentum q_T of the virtual photon. However, the leptonic tensor $L^{\mu\nu}$ clearly will depend on this transverse momentum, making a clean separation between leptonic and hadronic parts impossible. A common procedure is then to change frame in such a way that this separation is possible [19, 20, 2].
ADD HERE DISCUSSION OF BOER03
It turns out that the Breit frame in which the virtual photon and the nucleon are

collinear is an appropriate choice. In this new frame, the photon momentum doesn't have a temporal component (which is possible since in SIDIS q^μ is always a space-like vector). The hadron momentum now acquires a perpendicular component. We then construct the Lorentz transformation from the PP_h frame to the Breit frame. It turns out to be

$$\Lambda^\mu_\nu = \begin{pmatrix} 1+\frac{Q_T^2}{2Q^2} & -\frac{Q_T}{Q}\cos\phi_q & -\frac{Q_T}{Q}\sin\phi_q & -\frac{Q_T^2}{2Q^2} \\ -\frac{Q_T}{Q}\cos\phi_q & 1 & 0 & \frac{Q_T}{Q}\cos\phi_q \\ -\frac{Q_T}{Q}\sin\phi_q & 0 & 1 & \frac{Q_T}{Q}\sin\phi_q \\ \frac{Q_T^2}{2Q^2} & -\frac{Q_T}{Q}\cos\phi_q & -\frac{Q_T}{Q}\sin\phi_q & 1-\frac{Q_T^2}{2Q^2} \end{pmatrix} \tag{2.12}$$

We note that this transformation satisfies the usual Lorentz transformation properties $\det\Lambda = 1$ and $\Lambda^T g \Lambda = g$. In this frame, the momenta read

$$\begin{aligned} P^\mu &= \Big(\frac{Q}{2x_B}, 0, 0, \frac{Q}{2x_B}\Big) \\ P_h^\mu &= \frac{z_h Q}{2}\Big(1+\chi_T^2, -2\chi_T\cos\phi_q, -2\chi_T\sin\phi_q, -1+\chi_T^2\Big) \\ q^\mu &= \Big(0,0,0,-Q\Big) \\ l^\mu &= \frac{Q}{2}\Big(\frac{2-y}{y}, \frac{2}{y}\sqrt{1-y}\cos\phi_l, \frac{2}{y}\sqrt{1-y}\sin\phi_l, -1\Big) \\ l'^\mu &= \frac{Q}{2}\Big(\frac{2-y}{y}, \frac{2}{y}\sqrt{1-y}\cos\phi_l, \frac{2}{y}\sqrt{1-y}\sin\phi_l, +1\Big) \end{aligned} \tag{2.13}$$

where ϕ_l is an azimuthal angle around the z-axis [13]. A sketch of the lepton and hadron planes, along with the conventions for the different angles is shown in Fig. 2.2. It turns out that our results are particularly simple when expressed in terms of the difference $\phi_S - \phi_l$, where ϕ_S is the azimuthal angle of the transverse spin vector $\boldsymbol{S}_\perp$ of the nucleon. In fact, one can define such angle through the following Lorentz-invariant expression, adhering to the Trento conventions [3]

$$\begin{aligned} \sin(\phi_S-\phi_l) &= -\frac{\epsilon_\perp^{\mu\nu} l_\mu S_\nu}{\sqrt{-g_\perp^{\mu\nu} l_\mu l_\nu}} = -\frac{2x_B y}{Q^3\sqrt{1-y}}\epsilon^{lPqS} = +\frac{2x_B y}{Q^3\sqrt{1-y}}\epsilon^{lPl'S} \\ \cos(\phi_S-\phi_l) &= -\frac{g_\perp^{\mu\nu} l_\mu S_\nu}{\sqrt{-g_\perp^{\mu\nu} l_\mu l_\nu}} = \frac{y}{Q\sqrt{1-y}}(\text{TO CHECK}) \end{aligned} \tag{2.14}$$

with the transverse Levi-Civita tensor defined as $\epsilon_\perp^{\mu\nu} = \epsilon^{\rho\sigma\mu\nu} P_\rho P_{h\sigma}/(P\cdot P_h)$. We note that the definition of ϕ_S is frame independent, as it should be.

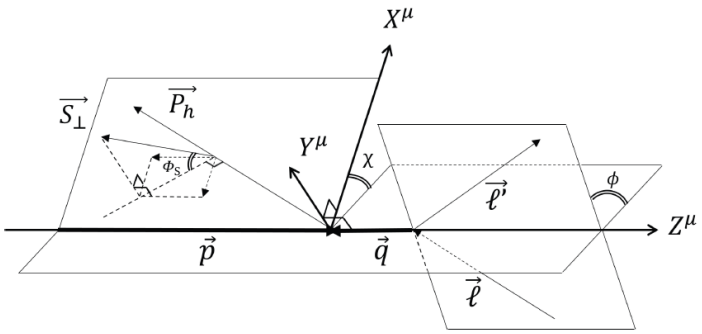

Figure 2.2: The Breit frame. The virtual photon and the nucleon are collinear along the z axis. In this frame, the hadron momentum P_h acquires a transverse component. The lepton momenta l, l' lie in the lepton plane, which forms an angle ϕ_l with respect to the hadron production plane. The transverse spin vector $\boldsymbol{S}_\perp$ of the nucleon forms an angle ϕ_S with respect to the lepton plane.

Also, the partonic momenta now become

$$\begin{aligned} k^\mu &= xP^\mu + k_T^\mu \Big|_{\text{BF}} = xP^\mu + \vec{k}_\perp^\mu + 2x_B \frac{\vec{k}_\perp^2}{Q^2} P^\mu \\ p^\mu &= \frac{1}{z} P_h^\mu + p_T^\mu \Big|_{\text{BF}} = \frac{1}{z} P_h^\mu + \vec{p}_\perp^\mu - 2x_B \frac{\vec{p}_\perp^2}{Q^2} P^\mu \end{aligned} \tag{2.15}$$

where P and P_h are in the Breit frame, of course. We anticipate that at LO, after integration, the momentum of the detected hadron can be written as

$$P_h^\mu = z_h(x_B P^\mu + q^\mu) + z_h x_B \frac{(\vec{k}_\perp - \vec{p}_\perp)^2}{Q^2} P^\mu + z_h(\vec{k}_\perp - \vec{p}_\perp)^\mu. \tag{2.16}$$

Accordingly, one of the light cone vectors remain unchanged $m^\mu \to m^\mu = \frac{2x_B}{z_h Q^2} P^\mu$ while the other is modified $n^\mu \to n^\mu = \frac{2x_B}{Q^2}(x_B P^\mu + q^\mu) + \mathcal{O}(k_\perp, p_\perp)$. We note the important fact that in one frame transverse 4-momenta are actually just 2-dimensional vectors, but in the Breit frame the perpendicular 4-vector also acquires a component in the + direction due to the Lorentz transformation. This will play a fundamental role in the emergence of twist-3 effects, since this correction in the + direction is only $1/Q$ suppressed. Furthermore, it is clear that the temporal and z directions are determined

by the momenta P and q. It makes sense to introduce another projector

$$g_\perp^{\mu\nu} = g^{\mu\nu} - \frac{1}{P\cdot q}[P^\mu(q+x_B P)^\nu + P^\nu(q+x_B P)^\mu], \tag{2.17}$$

which has the same role of projecting out the perpendicular components but now in the Breit frame. We note the important fact that $g_\perp^{\mu\nu}$ acquires the same form as $g_T^{\mu\nu}$, thus justifying the frequent SIDIS identification $\vec{P}_{h\perp} = -z_h\vec{q}_T$. Also, the transformation leaves the perpendicular/transverse component invariant, so we can identify simply $\vec{k}_T = \vec{k}_\perp$ and $\vec{p}_T = \vec{p}_\perp$ where $\vec{a}_T = (a_1, a_2)$. This is true for the 2-dimensional transverse vector but, again, not at the level of 4-vectors. In the Breit frame, the meaning of the integration over $\vec{P}_{h\perp}$ is now clear. We note that the leptonic part is now independent of $\vec{P}_{h\perp}$ and it can be separated from hadronic component.

From now on, we carry on the calculation in the Breit frame. Going back to Eq. (2.8) and performing the Lorentz transformation we get the following Jacobian factors

$$\begin{aligned}\frac{\mathrm{d}^3 l'}{2E'} &= J_l \mathrm{d}x_B \mathrm{d}y \mathrm{d}\phi_l,\\ \frac{\mathrm{d}^3 P_h}{2E_h} &= J_{P_h} \mathrm{d}z_h \mathrm{d}^2 P_{h\perp},\end{aligned} \tag{2.18}$$

with $J_l = Q^2/4x_B$ and $J_{P_h} = 1/2z_h$. The flux factor is given by $F = 2s$, where $s = (l+P)^2 = Q^2/x_B y$ is the common center-of-mass energy squared. The $P_{h\perp}$-integrated cross section is therefore given by

$$\frac{\mathrm{d}\sigma}{\mathrm{d}x_B \mathrm{d}y \mathrm{d}\phi_l \mathrm{d}z_h} = \frac{J_l J_{P_h} (4\pi)^2 \alpha_{\mathrm{em}}^2}{2sQ^4(2\pi)^{d-2}} L^{\mu\nu} \int \mathrm{d}^{d-2} P_{h\perp} W_{\mu\nu}. \tag{2.19}$$

ADD STUFF HERE ON DETAILS OF DERIVATION

2.1.1 Results

Following the prescription outlined above, we derive the LO SIDIS cross section in the unpolarized nucleon case, as well as the transversely polarized proton case. We remark

that the produced hadron $h(P_h)$ is always assumed to be unpolarized. The result is

$$\begin{aligned}\frac{\mathrm{d}\sigma_{UU}}{\mathrm{d}x_B\mathrm{d}y\mathrm{d}\phi_l\mathrm{d}z_h} &= \frac{2\alpha_{\mathrm{em}}^2}{yQ^2}\left[\left(1-y+\frac{y^2}{2}\right)F_{UU,T}\right]+\mathcal{O}(\alpha_S),\\ \frac{\mathrm{d}\sigma_{UT}(\boldsymbol{S}_\perp)}{\mathrm{d}x_B\mathrm{d}y\mathrm{d}\phi_l\mathrm{d}z_h} &= \frac{2\alpha_{\mathrm{em}}^2}{yQ^2}\left[|\boldsymbol{S}_\perp|(2-y)\sqrt{1-y}\sin(\phi_S-\phi_l)F_{UT}^{\sin\phi_S}\right]+\mathcal{O}(\alpha_S),\end{aligned} \tag{2.20}$$

with the leading order unpolarized and polarized structure functions

$$\begin{aligned}F_{UU,T} &= \sum_a e_a^2\, f_1^a(x_B)\, D_1^a(z_h),\\ F_{UT}^{\sin\phi_S} &= \frac{2M_h}{Q}\sum_a e_a^2\, h_1^a(x_B)\,\frac{\tilde{H}^a(z_h)}{z_h}.\end{aligned} \tag{2.21}$$

ADD DEPOLAIRZATION EPSILONS CONVENTION!!!
The result derived here is perfectly consistent with the literature [20, 2] up to a overall sign, which is due to the fact that we are using a frame in which the z axis is reversed (and hence ϕ_S is opposite) compared to similar calculations found in the literature. The spin-dependent cross section in the result in Eq. 2.20 is obtained by collecting the intrinsic ($\sim H$), kinematical ($\sim H_1^{\perp(1)}$) and dynamical ($\sim \int \mathrm{Im}[\hat{H}_{FU}]$) contributions and combining them via the QCD equation of motion. Interestingly, the final UT cross section can be expressed solely in terms of quark-gluon-quark correlation functions. In this sense we can conclude that, at least at leading order in α_S, intrinsic and kinematical functions are auxiliary objects in favor of more general and complicated QGQ correlation functions. Overall, the transverse spin asymmetry for this polarization case is easily obtained

$$A_{UT} = \frac{\sigma_{UT}(\boldsymbol{S}_\perp)-\sigma_{UT}(-\boldsymbol{S}_\perp)}{\sigma_{UT}(\boldsymbol{S}_\perp)+\sigma_{UT}(-\boldsymbol{S}_\perp)} = \frac{\sigma_{UT}}{\sigma_{UU}} = \frac{2M_h(2-y)\sqrt{1-y}}{Q(1-y+\frac{y^2}{2})}\frac{\sum_a e_a^2 h_1^a(x_B)\tilde{H}^a(z_h)/z_h}{\sum_a e_a^2 f_1^a(x_B)D_1^a(z_h)} \tag{2.22}$$

The next sections of this work are dedicated to the calculation of NLO corrections contributing to the A_{UT} transverse spin asymmetry. The NLO unpolarized cross section gives corrections to the denominator of the asymmetry. On the other hand, the NLO polarized cross section gives corrections to the numerator of the asymmetry.

2.1.2 old stuff/material

$$\begin{aligned}\mathrm{d}\sigma^{q\to q} =&\frac{1}{F}\frac{\mathrm{d}^3 l'}{(2\pi)^3 2E'}\frac{\mathrm{d}^3 P_h}{(2\pi)^3 2E_h}\int \mathrm{d}^4k \int \mathrm{d}^4p\,(2\pi)^4\delta^{(4)}(q+k-p)\\ &\times \bar{\sum_{\text{spin,color}}} \mathrm{Tr}\Big[\hat{\mathcal{A}}^{q\to q}(k,p,q)\Phi(k)\hat{\bar{\mathcal{A}}}^{q\to q}(k,p,q)\Delta(p)\Big]\end{aligned} \tag{2.23}$$

In order to be as general as possible, we perform the calculation in d-dimensions, so that our LO result is readily extendable to a NLO one. Performing the $\mathrm{d}k^-$ and $\mathrm{d}p^+$ integrations we get

$$\begin{aligned}\mathrm{d}\sigma^{q\to q} =&\frac{2x_B z_h}{FQ^2(2\pi)^{d-2}}\frac{\mathrm{d}^{d-1}l'}{2E'}\frac{\mathrm{d}^{d-1}P_h}{2E_h}\int \mathrm{d}x \int \mathrm{d}^{d-2}k_T \int \frac{\mathrm{d}z}{z^2}\int \mathrm{d}^{d-2}p_T\\ &\times \delta(x-x_B(1-\chi_T^2))\delta(z-z_h)\delta^{(d-2)}(\vec{q}_T+\vec{k}_T-\vec{p}_T)\\ &\times \bar{\sum_{\text{spin,color}}} \mathrm{Tr}\Big[\hat{\mathcal{A}}^{q\to q}(k,p,q)\Phi(x,k_T)\hat{\bar{\mathcal{A}}}^{q\to q}(k,p,q)\Delta(z,p_T)\Big]\end{aligned} \tag{2.24}$$

where we now the TMD correlators appear. We stress that the separation of the delta function in such a way makes sense only in a frame where the nucleon and the hadron are collinear. In this case, the transverse vectors are indeed 2-dimensional and this kind of $(+,-,T)$ separation makes sense.

The $P_{h\perp}$-integrated cross section in the Breit frame reads

$$\begin{aligned}\frac{\mathrm{d}\sigma^{q\to q}}{\mathrm{d}x_B\mathrm{d}y\mathrm{d}\phi_l\mathrm{d}z_h} =&\frac{x_B z_h J_l J_{P_h}}{sQ^2(2\pi)^{d-2}}\int \mathrm{d}^{d-2}P_{h\perp}\int \mathrm{d}x\int \mathrm{d}^{d-2}k_\perp \int\frac{\mathrm{d}z}{z^2}\int \mathrm{d}^{d-2}p_\perp\\ &\times \delta\Big(x-x_B\big(1-\frac{\vec{P}_{h\perp}^2}{z_h^2Q^2}\big)\Big)\delta(z-z_h)\delta^{(d-2)}\Big(-\frac{\vec{P}_{h\perp}}{z_h}+\vec{k}_\perp-\vec{p}_\perp\Big)\\ &\times \bar{\sum_{\text{spin,color}}} \mathrm{Tr}\Big[\hat{\mathcal{A}}^{q\to q}(k,p,q)\Phi(x,k_\perp)\hat{\bar{\mathcal{A}}}^{q\to q}(k,p,q)\Delta(z,p_\perp)\Big]\Big|_{\chi_T^2=\frac{\vec{P}_{h\perp}^2}{z_h^2Q^2}}\end{aligned} \tag{2.25}$$

where we substituted the transverse 2-d vectors with the perpendicular ones and all the momenta are given in Eq. (2.13) and (2.15). Also, the important identification $\vec{P}_{h\perp}=-z_h\vec{q}_T$ has been used. For convenience, we isolate from the amplitude $\hat{\mathcal{A}}$ the

$\gamma(q) + q(k) \to q(p)$ Dirac vertex (without charge factors) which we denote by $\hat{\mathcal{M}}$. It is

$$\begin{aligned}&\bar{\sum_{\text{spin,color}}} \operatorname{Tr}\Big[\hat{\mathcal{A}}^{q\to q}(k,p,q)\Phi(k)\hat{\bar{\mathcal{A}}}^{q\to q}(k,p,q)\Delta(p)\Big]\\ &= \frac{(4\pi)^2\alpha_{\text{em}}^2}{Q^4}L^{\mu\nu}e_a^2\operatorname{Tr}\Big[\hat{\mathcal{M}}_\mu^{q\to q}(k,p,q)\Phi^a(k)\hat{\bar{\mathcal{M}}}_\nu^{q\to q}(k,p,q)\Delta^a(p)\Big]\end{aligned} \tag{2.26}$$

with the leptonic tensor defined as

$$L^{\mu\nu} = \frac{1}{2}\operatorname{Tr}\Big[(1+\lambda_e\gamma_5)\not{l}\gamma^\nu\not{l}'\gamma^\mu\Big] \tag{2.27}$$

where λ_e denotes the helicity of the incoming lepton. For a unpolarized lepton beam, simply $\lambda_e = 0$. In this frame, we can pull out the leptonic tensor from the transverse momentum integral, allowing us to have a clear separation between leptonic and hadronic part. This is exactly what we wanted to achieve with the Lorentz transformation. We introduce the hadronic tensor as

$$\begin{aligned}W_{\mu\nu}^{q\to q} &= e_a^2\int \mathrm{d}^d k\int \mathrm{d}^d p\,\delta^{(d)}(q+k-p)\operatorname{Tr}\Big[\hat{\mathcal{M}}_\mu^{q\to q}\Phi^a(k)\hat{\bar{\mathcal{M}}}_\nu^{q\to q}\Delta^a(p)\Big]\\ &= \frac{e_a^2 2x_B z_h}{Q^2}\int \mathrm{d}x\int \mathrm{d}^{d-2}k_\perp\int\frac{\mathrm{d}z}{z^2}\int \mathrm{d}^{d-2}p_\perp\,\delta\Big(x - x_B\big(1-\frac{\vec{P}_{h\perp}^2}{z_h^2Q^2}\big)\Big)\delta(z-z_h)\\ &\times\delta^{(d-2)}\Big(-\frac{\vec{P}_{h\perp}}{z_h}+\vec{k}_\perp-\vec{p}_\perp\Big)\operatorname{Tr}\Big[\hat{\mathcal{M}}_\mu^{q\to q}(k,p,q)\Phi^a(x,k_\perp)\hat{\bar{\mathcal{M}}}_\nu^{q\to q}(k,p,q)\Delta^a(z,p_\perp)\Big]\end{aligned} \tag{2.28}$$

such that the cross section is now factorized as

$$\boxed{\frac{\mathrm{d}\sigma}{\mathrm{d}x_B\mathrm{d}y\mathrm{d}\phi_l\mathrm{d}z_h} = \frac{J_l J_{P_h}(4\pi)^2\alpha_{\text{em}}^2}{2sQ^4(2\pi)^{d-2}}L^{\mu\nu}\int \mathrm{d}^{d-2}P_{h\perp}W_{\mu\nu}} \tag{2.29}$$

Performing the integration over the transverse momentum is now straightforward [1]

$$\begin{aligned}\int \mathrm{d}^{d-2}P_{h\perp}W_{\mu\nu}^{q\to q} = \frac{e_a^2 2x_B z_h}{Q^2} z_h^{2-2\epsilon}\int \mathrm{d}x \int \mathrm{d}^{d-2}k_\perp \int \frac{\mathrm{d}z}{z^2}\int \mathrm{d}^{d-2}p_\perp \\ \times \delta\Big(x - x_B\Big(1-\frac{(\vec{k}_\perp-\vec{p}_\perp)^2}{Q^2}\Big)\Big)\delta(z-z_h) \\ \times \mathrm{Tr}\Big[\hat{\mathcal{M}}_\mu^{q\to q}(k,p,q)\Phi^a(x,k_\perp)\hat{\bar{\mathcal{M}}}_\nu^{q\to q}(k,p,q)\Delta^a(z,p_\perp)\Big]\Big|_{\chi_T^2=\frac{(\vec{k}_\perp-\vec{p}_\perp)^2}{Q^2}}\end{aligned} \tag{2.30}$$

Performing the x and z integrations is also easy

$$\begin{aligned}\int \mathrm{d}^{d-2}P_{h\perp}W_{\mu\nu}^{q\to q} = \frac{e_a^2 2x_B z_h}{Q^2} z_h^{-2\epsilon}\int \mathrm{d}^{d-2}k_\perp \int \mathrm{d}^{d-2}p_\perp \\ \times \mathrm{Tr}\Big[\hat{\mathcal{M}}_\mu^{q\to q}(\bar{k},\bar{p},q)\Phi^a(\bar{x}_B,k_\perp)\hat{\bar{\mathcal{M}}}_\nu^{q\to q}(\bar{k},\bar{p},q)\Delta^a(z_h,p_\perp)\Big]\end{aligned} \tag{2.31}$$

where the bar prescription for the momenta really just means

$$\bar{a}^\mu = a^\mu\Big|_{\chi_T^2=\frac{(\vec{k}_\perp-\vec{p}_\perp)^2}{Q^2},x=\bar{x}_B,z=z_h} \tag{2.32}$$

with $\bar{x}_B = x_B\Big(1-\frac{(\vec{k}_\perp-\vec{p}_\perp)^2}{Q^2}\Big)$. At this point, we should not forget that the TMD correlators are themselves functions of P and P_h. Therefore their parametrization will be affected by the Lorentz transformation. This is particularly important since, the additional terms due to the change of frame give rise to twist-3 effects that wouldn't be taken into account otherwise. Schematically we have

$$\begin{aligned}\Phi(x,k_T) &\longrightarrow \Phi(\bar{x}_B,k_\perp|P,\bar{n}) \\ \Delta(z,p_T) &\longrightarrow \Delta(z_h,p_\perp|\bar{P}_h,m)\end{aligned} \tag{2.33}$$

In order to extract the genuine and kinematical twist-3 contribution we perform the

[1] Here, we use $\delta^{(d-2)}(\vec{P}_{h\perp}/z_h+\vec{k}_\perp-\vec{p}_\perp) = z_h^{2-2\epsilon}\delta^{(d-2)}(\vec{P}_{h\perp}-z_h(\vec{k}_\perp-\vec{p}_\perp))$, where we set $d=4-2\epsilon$.

so-called collinear expansion of the hard scattering part

$$\boxed{\begin{aligned}\int \mathrm{d}^{d-2}P_{h\perp}W^{q\to q}_{\mu\nu} = \frac{e_a^2 2x_B z_h}{Q^2} z_h^{-2\epsilon}\int \mathrm{d}^{d-2}k_\perp \int \mathrm{d}^{d-2}p_\perp \\ \times \mathrm{Tr}\left[\left(\hat{\mathcal{M}}^{q\to q}\Big|_{\mathrm{CL}} + k_\perp^\alpha \frac{\partial \hat{\mathcal{M}}^{q\to q}}{\partial k_\perp^\alpha}\Big|_{\mathrm{CL}} + p_\perp^\alpha \frac{\partial \hat{\mathcal{M}}^{q\to q}}{\partial p_\perp^\alpha}\Big|_{\mathrm{CL}}\right)_\mu \Phi(\bar{x}_B, k_\perp|P,\bar{n}) \\ \times \left(\hat{\bar{\mathcal{M}}}^{q\to q}\Big|_{\mathrm{CL}} + k_\perp^\alpha \frac{\partial \hat{\bar{\mathcal{M}}}^{q\to q}}{\partial k_\perp^\alpha}\Big|_{\mathrm{CL}} + p_\perp^\alpha \frac{\partial \hat{\bar{\mathcal{M}}}^{q\to q}}{\partial p_\perp^\alpha}\Big|_{\mathrm{CL}}\right)_\nu \Delta(z_h, p_\perp|\bar{P}_h, m)\right]\end{aligned}} \tag{2.34}$$

In order to include dynamical twist-3 effects, we shall include the $q \to gq$ and $qg \to q$ diagrams as interference with the collinear $q \to q$ diagram. In this case, we can drop perpendicular momenta right from the beginning and easily obtain a collinear factorization formula. Considering these contributions, we get

$$\begin{aligned}\int \mathrm{d}^{d-2}P_{h\perp}W^{q\to gq+qg\to q}_{\mu\nu} = \frac{e_a^2 2x_B z_h}{Q^2} z_h^{-2\epsilon}\Bigg(\int \mathrm{d}x'\,\mathrm{Tr}\left[\frac{\hat{\mathcal{M}}^{qg\to q}_{\mu\rho}}{g_S T^\alpha}\Phi^\rho_A(x_B,x')\hat{\bar{\mathcal{M}}}^{q\to q}_\nu \Delta(z_h)\right] + \text{c.c.} \\ + \int \frac{\mathrm{d}z'}{z'^2}\,\mathrm{Tr}\left[\frac{\hat{\mathcal{M}}^{q\to gq}_{\mu\rho}}{g_S T^\alpha}\Phi(x_B)\hat{\bar{\mathcal{M}}}^{q\to q}_\nu \Delta^\rho_A(z_h,z')\right] + \text{c.c.}\Bigg)\end{aligned} \tag{2.35}$$

where in the dynamical correlators we absorbed a factor of $g_s T^\alpha$ from the Feynman amplitude

$$\begin{aligned}\Phi^\rho_A(x,x') &= \int \frac{\mathrm{d}\xi^-}{2\pi}\frac{\mathrm{d}\zeta^-}{2\pi} e^{ix'\xi^- + i(x-x')\zeta^-}\,\langle PS|\bar{\psi}(0) g_S G^\rho(\zeta)\psi(\xi)|PS\rangle \\ \Delta^\rho_A(z,z') &= \int \mathrm{d}\Pi_X \int \frac{\mathrm{d}\xi^+}{2\pi}\frac{\mathrm{d}\zeta^+}{2\pi} e^{-i\frac{\xi^+}{z'} - i(\frac{1}{z}-\frac{1}{z'})\zeta^+}\,\langle 0|\psi(0)|P_h,X\rangle\,\langle P_h,X|g_S G^\rho(\zeta)\bar{\psi}(\xi)|0\rangle\end{aligned} \tag{2.36}$$

Here, the gauge field does not carry an adjoint SU(N) index since it is intended to be already traced with the generators

$$G^\mu(x) \equiv G^{\mu,\alpha}(x)T^\alpha \tag{2.37}$$

In light-cone gauge $m \cdot A = 0$, we have that for the gluon field-strength tensor it holds

$$m_\mu G^{\mu\nu} = m_\mu(\partial^\mu G^\nu - \partial^\nu G^\mu + g_S T^\alpha C^{\alpha\beta\gamma} G^{\mu,\beta} G^{\nu,\gamma}) = m\cdot\partial G^\nu = \frac{\partial}{\partial\zeta^+}G^\nu \tag{2.38}$$

Therefore, assuming sufficiently fast vanishing gluon fields at the boundaries (or asymmetric boundary conditions), we can integrate by parts and pull down, for example, a factor $1/z - 1/z'$ from the exponential. Schematically

$$\int \mathrm{d}\zeta^+ e^{-i(\frac{1}{z}-\frac{1}{z'})\zeta^+} \left\langle ig_S \frac{\partial}{\partial\zeta^+} G^\rho(\zeta) \right\rangle = (\text{boundary-term}) \\ - (-i)\left(\frac{1}{z}-\frac{1}{z'}\right)\int \mathrm{d}\zeta^+ e^{-i(\frac{1}{z}-\frac{1}{z'})\zeta^+} \langle ig_S G^\rho(\zeta)\rangle \tag{2.39}$$

therefore, if we include a factor of i into Δ_F but not in Δ_A we get

$$\Delta_A^\rho(z,z') = -\frac{1}{\frac{1}{z}-\frac{1}{z'}}\Delta_F^\rho(z,z') \tag{2.40}$$

Furthermore, in twist-3 fragmentation, only transverse gluons has to be taken into account in the end [4], since

$$G^\mu = \underbrace{(m\cdot G)}_{=0} P_h^\mu + \underbrace{(P_h\cdot G)}_{\text{twist-4}} m^\mu + G_\perp^\mu \approx G_\perp^\mu = G_\nu g_\perp^{\mu\nu} \tag{2.41}$$

We can then use the useful mapping relevant for dynamical twist-3 fragmentation terms

$$\Delta_A^\rho(z,z')\hat{\mathcal{M}}_{\mu\rho}^{q\to gq} \to -\frac{\Delta_F^\rho(z,z')}{\frac{1}{z}-\frac{1}{z'}}\hat{\mathcal{M}}_{\mu}^{q\to gq,\nu} g_{\perp\rho\nu} \tag{2.42}$$

where Δ_F denotes the gluon field-strength correlator. One can also show this kind of arrangement in Feynman gauge (see notes on draft Kanazawa16, 6.3). This mapping is also applicable on the distribution side, with the usual symmetry $x \leftrightarrow 1/z$. Note that we get a different sign for the distribution mapping since the exponential factors in Eq. 2.36 have different signs. We get

$$\Phi_A^\rho(x,x')\hat{\mathcal{M}}_{\mu\rho}^{qg\to q} \to \frac{\Phi_F^\rho(x,x')}{x-x'}\hat{\mathcal{M}}_{\mu}^{qg\to q,\nu} g_{\perp\rho\nu} \tag{2.43}$$

The hadronic tensor involving the dynamical terms is therefore

$$\boxed{\begin{aligned}\int \mathrm{d}^{d-2}P_{h\perp}W_{\mu\nu}^{q\to gq+qg\to q} &= \frac{e_a^2 2x_B z_h}{Q^2} z_h^{-2\epsilon} \\ &\times \left(\int_0^{x_B} \mathrm{d}x' \frac{1}{x_B - x'} \,\mathrm{Tr}\left[\frac{\hat{\mathcal{M}}_\mu^{qg\to q,\rho}}{g_S T^\alpha} \Phi_F^\sigma(x_B, x') \hat{\bar{\mathcal{M}}}_\nu^{q\to q} \Delta(z_h) \right] g_{\perp\rho\sigma} + \text{c.c.} \right. \\ &\left. + \int_{z_h}^\infty \frac{\mathrm{d}z'}{z'^2} \frac{(-1)}{\frac{1}{z_h} - \frac{1}{z'}} \,\mathrm{Tr}\left[\frac{\hat{\mathcal{M}}_\mu^{q\to gq,\rho}}{g_S T^\alpha} \Phi(x_B) \hat{\bar{\mathcal{M}}}_\nu^{q\to q} \Delta_F^\sigma(z_h, z') \right] g_{\perp\rho\sigma} + \text{c.c.} \right)\end{aligned}} \tag{2.44}$$

Note that it is quite common to perform a change of variables in the fragmentation part introducing the scaled variable $\zeta \equiv z_h/z'$. Then the integration arranges as

$$\int_{z_h}^\infty \frac{\mathrm{d}z'}{z'^2} \frac{\Delta(z_h, z')}{1/z_h - 1/z'} h(z') = \int_0^1 \mathrm{d}\zeta \frac{\Delta\left(z_h, z_h/\zeta\right)}{1-\zeta} h(z_h/\zeta) \tag{2.45}$$

Chapter 3

Next-to-Leading Order QCD Analysis of the spin asymmetry

We perform our pQCD calculation at next-to-leading order in dimensional regularization in $d = 4-2\epsilon$ dimensions. When it comes to renormalization, we adopt the common choice of using the modified minimal subtraction scheme ($\overline{\text{MS}}$).

3.1 Leading-twist case

The virtual graphs contributing at twist-2 level are shown in Fig.3.1. Since we are

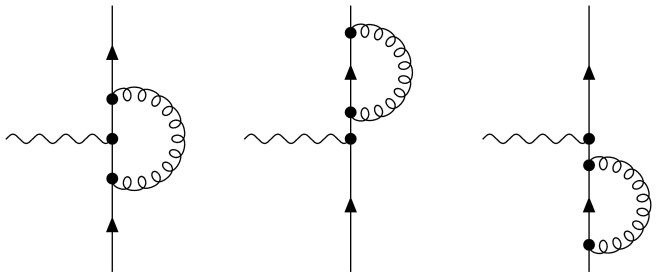

Figure 3.1: Virtual diagrams contributing to the leading-twist unpolarized cross section at NLO.

performing our pQCD calculation in light-cone gauge, we shall employ an appropriate technique to evaluate loop integrals that allows us to treat the denominator of the gluon propagator in this gauge. Notoriously, this $(r\cdot m)^{-1}$ term requires a careful treatment since it may lead to additional well-known *light-cone divergences*, i.e. when $r\cdot m\to 0$. Not surprisingly, it turns out that a light-cone decomposition of the loop momentum allows for a systematic procedure to integrate out the $+$, $-$ and perpendicular components. Since this technique is essential for calculating virtual corrections also at the twist-3 level, we present it here in detail for the simpler leading-twist case. The method is quite general and can be readily extended to higher-twist contributions. Let's start by calculating the vertex correction graph. The amplitude reads

$$\begin{aligned}(\hat{\mathcal{M}}^{q\to q}_{\text{NLO,vir}})^{\mu}_{ij,ac} &= \int \frac{\mathrm{d}^d r}{(2\pi)^d}\frac{\tilde{N}^{\mu}_{ij,ac}(r)}{[(p-r)^2+i\delta][(k-r)^2+i\delta][r^2+i\delta]r\cdot m},\\ \tilde{N}^{\mu}_{ij,ac}(r) &\equiv -ig_S^2\mu^{4-d}T^{\alpha}_{ab}T^{\beta}_{bc}\delta_{\alpha\beta}\left[\gamma^{\lambda}(\not{p}-\not{r})\gamma^{\mu}(\not{k}-\not{r})\gamma^{\eta}\right]_{ij}\left[(r\cdot m)g_{\lambda\eta}-\kappa r_{(\lambda}m_{\eta)}\right].\end{aligned} \tag{3.1}$$

As already anticipated, it is convenient to express the loop momentum in its light-cone decomposition $r^{\mu}=\alpha P_h^{\mu}+\beta m^{\mu}+r_{\perp}^{\mu}$ with $\alpha\equiv r\cdot m$ and $\beta\equiv r\cdot P_h$. By doing this, given a generic momentum p_j, the denominator of the propagators become of the form

$$(p_j-r)^2+i\delta=(2\alpha-2p_j\cdot m)(\beta-\beta_j),\qquad \beta_j\equiv-\frac{r_{\perp}^2+p_j^2-2\alpha\, p_j\cdot P_h+i\delta}{2\alpha-2p_j\cdot m} \tag{3.2}$$

In order to simplify the calculation, we find that it is convenient to perform the integration at the level of the hadronic tensor, and not just the amplitude alone. This is because many terms that are present in the hard scattering amplitude $\hat{\mathcal{M}}$ may vanish when traced with correlators and the LO interfering amplitude. We have then

$$\begin{aligned}(W^{q\to q}_{\text{NLO,vir}})^{\mu\nu} &= \int_{-\infty}^{+\infty}\frac{\mathrm{d}\alpha}{2\pi}\frac{1}{2\alpha(2\alpha-2p\cdot m)(2\alpha-2k\cdot m)\alpha}\int\frac{\mathrm{d}^{d-2}r_{\perp}}{(2\pi)^{d-2}}\\ &\quad\times\int_{-\infty}^{+\infty}\frac{\mathrm{d}\beta}{2\pi}\frac{N^{\mu\nu}(\alpha,r_{\perp},\beta)}{(\beta-\beta_0)(\beta-\beta_1)(\beta-\beta_2)},\\ N^{\mu\nu} &\equiv \frac{e_a^2 2x_B z_h}{Q^2}z_h^{-2\epsilon}\,\mathrm{Tr}\Big[\tilde{N}^{\mu}\Phi^a\gamma^{\nu}\Delta^a\Big].\end{aligned} \tag{3.3}$$

By studying the position of the poles β_j $(j=0,1,2)$ in the complex plane, we can use contour integration and the residue theorem to evaluate the β integral in a straightforward manner. In order to perform the integration in this way, the integrand should

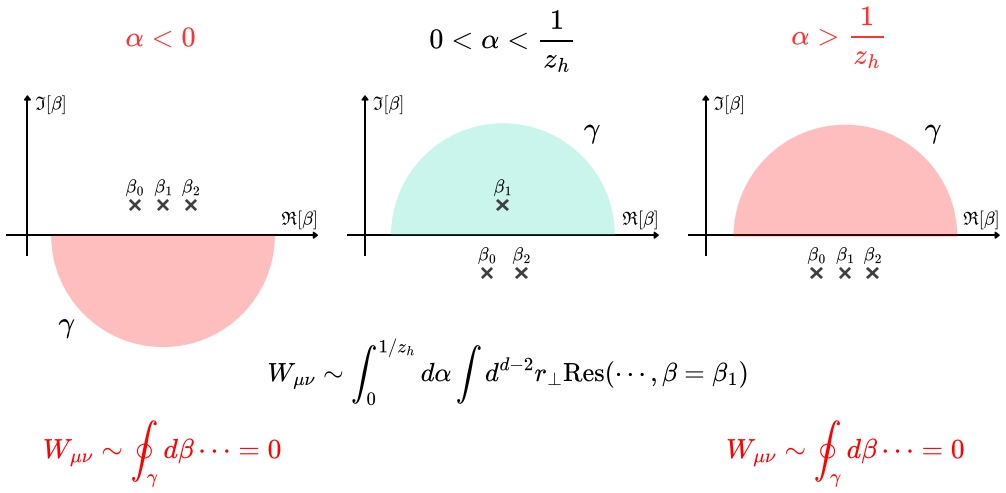

Figure 3.2: Sketch of the light-cone contour integration technique used for calculating virtual graphs in this work. Poles placements are studied and non-vanishing contributions to the hadronic tensor are identified with the residue theorem.

fall off at least as $\sim 1/\beta$ for large β (meaning that $N^{\mu\nu}$ should be at most quadratic in β, which turns out to be the case). Evidently, the poles β_j depend on α, as seen in Eq. (3.2). In particular, the pole will lay above or below the real axis depending on the sign of $2\alpha - 2p_j \cdot m$. By studying the imaginary part of all poles we can conveniently close the contour above or below the real axis and obtain the non-vanishing contributions to the β integral. This, in turn, restricts the domain of integration over α, since for certain values of α all the poles lie above (below) the real axis and we can close the contour below (above) and obtain zero since the curve does not include any poles. Going back to the integral above, we find that it is non-vanishing only for $0 < \alpha < 1/z_h$, and the only relevant pole is $\beta_1 = -(r_\perp^2 + i\delta)/2(\alpha - 1/z_h)$. A graphical sketch of the contour integration procedure can be found in Fig. 3.2. We then have

$$
\begin{aligned}
(W^{q\to q}_{\mathrm{NLO,vir}})^{\mu\nu} = \int_0^{1/z_h} \frac{\mathrm{d}\alpha}{2\pi} \frac{1}{2\alpha(2\alpha - 2p\cdot m)(2\alpha - 2k\cdot m)\alpha} \int \frac{\mathrm{d}^{d-2} r_\perp}{(2\pi)^{d-2}} \\
\times 2\pi i \,\mathrm{Res}\left[\frac{N^{\mu\nu}(\alpha, r_\perp, \beta)}{2\pi(\beta - \beta_0)(\beta - \beta_1)(\beta - \beta_2)}, \beta = \beta_1\right]
\end{aligned}
\tag{3.4}
$$

After β contour integration, the denominator factors arrange as $\beta_1 - \beta_j = C_{1j}(\vec{r}_\perp^2 + \omega_{1j}^2)$, with $j = 0, 2$ and C_{1j}, ω_{1j}^2 some functions of α. Then, the integration over the perpendicular loop momentum can be readily performed since the integrand depends only on the square modulus of $r_\perp$ (after dropping linear terms in the numerator since they vanish for symmetry). Adopting $d-2$ dimensional spherical coordinates, the angular integration is trivial and the radial integral turns out to be of the form

$$\int_0^\infty \mathrm{d}\rho \frac{\rho^{2n+1-2\epsilon}}{(\rho^2+\omega_1^2)(\rho^2+\omega_2^2)} = \frac{\pi}{2\sin(\pi n - \pi\epsilon)} \frac{(\omega_1^2)^{n-\epsilon} - (\omega_2^2)^{n-\epsilon}}{\omega_1^2 - \omega_2^2} \quad \text{if} \quad -1 < n - \epsilon < 1 \tag{3.5}$$

where $n \in \{\mathbb{N}, 0\}$ and assuming $\omega_1^2, \omega_2^2 > 0$. Hence, within this framework, divergences are regulated through the dimension of the $d-2$ dimensional perpendicular space. Lastly, the α integral can be evaluated by direct integration. We find that the hypergeometric function ${}_2F_1$ turns out to be quite useful in the evaluation of these α integrals. It can be expressed as [7]

$${}_2F_1(a, b, c; \xi) = \frac{\Gamma(c)}{\Gamma(b)\Gamma(c-b)} \int_0^1 \mathrm{d}\alpha \, (1-\alpha\xi)^{-a} \alpha^{b-1} (1-\alpha)^{c-b-1}, \tag{3.6}$$

if $\mathrm{Re}\, c > \mathrm{Re}\, b > 0$ and $|\xi| < 1$. It can be analytically be continued to the whole cut complex plane requiring $|\arg(1-\xi)| < \pi$. The expansion around integer parameters of ${}_2F_1$ can be easily performed with appropriate software [12]. Interestingly, the gauge dependence through the parameter κ completely drops out in the end, leaving us with a gauge invariant expression. We therefore have the result

$$\frac{\mathrm{d}\sigma^{UUU}_{\mathrm{NLO,vir}}}{\mathrm{d}x_B \mathrm{d}y \mathrm{d}\phi_l \mathrm{d}z_h} = \frac{\mathrm{d}\sigma^{UUU}_{\mathrm{LO}}}{\mathrm{d}x_B \mathrm{d}y \mathrm{d}\phi_l \mathrm{d}z_h} \times \frac{\alpha_S}{2\pi} C_F S_\epsilon \left(\frac{\mu^2}{Q^2}\right)^\epsilon \left(-\frac{2}{\epsilon^2} - \frac{3}{\epsilon} - 8\right) \tag{3.7}$$

with the common $\overline{\mathrm{MS}}$ scheme constant $S_\epsilon = (4\pi)^\epsilon/\Gamma(1-\epsilon)$. This in agreement with the original result for this γqq vertex correction [1].

In principle, we should also calculate two other diagrams, namely the self-energy corrections of the quark lines. Interestingly, if we repeat the very same procedure explained above, we find that after contour integration over β the denominator factor is proportional to $r_\perp^2$ only ($\omega_{ij}^2 = 0$) for both diagrams. This leads to a contribution that goes as

$$(\hat{\mathcal{M}}^{q\to q}_{\mathrm{NLO,vir,self\text{-}energy}})^\rho \sim \int \frac{\mathrm{d}^{d-2} r_\perp}{(2\pi)^{d-2}} \frac{A + B\, r_\perp^2}{r_\perp^2} \tag{3.8}$$

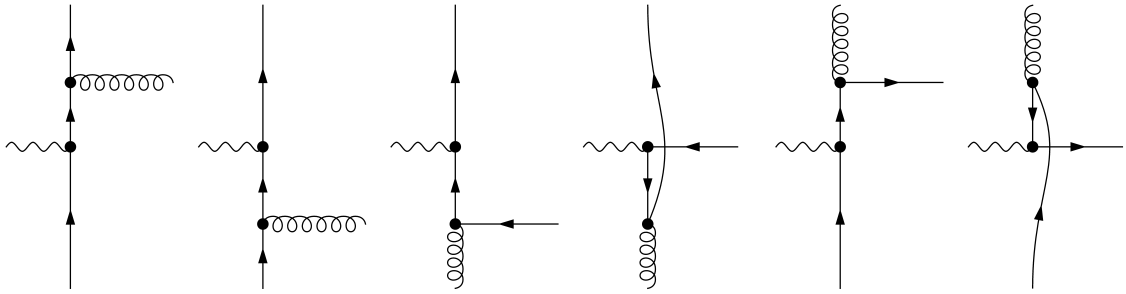

Figure 3.3: Real diagrams contributing to the leading-twist unpolarized cross section at NLO. All three partonic channels are shown: $q \to q$ channel (left), $g \to q$ channel (middle) and $q \to g$ channel (right).

which vanishes. This is because, in dimensional regularization, it is consistent to set to zero all scale-less integrals [22]. Therefore, the vertex correction is the only virtual diagram that has to be taken into account. Furthermore, this diagram leads to an hadronic tensor which is IR divergent only. No direct UV counterterms are then needed for this diagram (and for the two self-energy graphs, since they vanish). All in all, the full UV-renormalized virtual correction to the unpolarized cross section is just given by Eq. 3.7.

Another $\mathcal{O}(\alpha_S)$ correction to the cross section involves the emission of a final unobserved parton produced in the hard scattering process. At NLO, not only we can have the $q \to q$ channel (with real emission of gluons), but also $q \to g$ and $g \to q$ (with real emission of quarks). For all channels, the hadronic tensor is modified since there is an additional integration over the phase-space of the unobserved parton. The integrations in the hadronic tensors are modified according to

$$W^{\mu\nu}_{\text{NLO,real}} = \frac{e_a^2}{(2\pi)^{d-1}} \int \mathrm{d}^d k \int \mathrm{d}^d p \, \delta^+((q+k-p)^2) \, \mathrm{Tr}\Big[\hat{\mathcal{M}}^{\mu}_{\text{NLO}} \Phi^a \hat{\bar{\mathcal{M}}}^{\nu}_{\text{NLO}} \Delta^a\Big], \qquad (3.9)$$

where the momentum r^μ of the unobserved parton is set to $r = q + k - p$. We work again in the Breit frame as before. Integration over $\mathrm{d}k^-$ and $\mathrm{d}p^+$ is trivial. Here, since we are calculating the NLO corrections in the leading-twist unpolarized case, we can integrate over the transverse partonic momenta straight away. We are therefore left with integrations over the momentum fractions x and z. The delta function results in

the condition [17]

$$\delta^+((q+k-p)^2) = z z_h \delta\left(Q^2 z_h^2\Big(1-\frac{z}{z_h}\Big)\Big(1-\frac{x}{x_B}\Big) - \vec{P}_{h\perp}^2\right)\theta(q^0+k^0-p^0), \tag{3.10}$$

where the θ function restricts the kinematic variables in the following way WRONG

$$q^0+k^0-p^0 \geq 0 \iff \frac{x}{x_B} - \frac{z}{z_h}\left(1+\frac{Q_T^2}{Q^2}\right) \geq 0 \iff \frac{x}{x_B}+\frac{z}{z_h}-2 \geq 0. \tag{3.11}$$

Note that this condition would result in a complicated convolution of the x and z integrals due to the fact that the integration limits may depend on the other variable, i.e. the lower integration limits would result in either $z_{\min}(x)$ or $x_{\min}(z)$. However, one can greatly simplify the problem by simply ignoring the target fragmentation region, introducing a kinematical cut z_{cut} and x_{cut} [23] In this work, we simply set the kinematical cut $z_{\text{cut}} \approx z_h$ and $x_{\text{cut}} \approx x_B$. With this prescription, the integration variables must satisfy $z > z_h$ and $x > x_B$ and our formulae match many results already available in the literature [8, 16]. We note however that one can also fully keep the integration limits $x_{\min}$ and $z_{\min}$ as they are, like done in [13]. Nothing really changes in the end, except for the fact that the integration limits are more complicated and numerically they would probably result in a slightly different overall value for the integrals.
The hadronic tensor now reads

$$W_{\mu\nu}^{\text{NLO,real}} = \frac{e_a^2 z_h}{(2\pi)^{d-1}}\int_{x_B}^1 \mathrm{d}x \int_{z_h}^1 \frac{\mathrm{d}z}{z}\,\delta\left(Q^2 z_h^2\Big(1-\frac{z}{z_h}\Big)\Big(1-\frac{x}{x_B}\Big) - \vec{P}_{h\perp}^2\right) w_{\mu\nu}, \tag{3.12}$$

where, depending on the channel, $w_{\mu\nu}$ assumes different forms

$$\begin{aligned}
w_{\mu\nu}^{a,q\to q} &= \mathrm{Tr}\Big[\hat{\mathcal{M}}_{\mu}^{\text{NLO,real},q\to q}\Phi^a(x)\hat{\bar{\mathcal{M}}}_{\nu}^{\text{NLO,real},q\to q}\Delta^a(z)\Big],\\
w_{\mu\nu}^{a,g\to q} &= \Phi_g^{\lambda\eta}(x)\,\mathrm{Tr}\Big[\hat{\mathcal{M}}_{\mu\lambda}^{\text{NLO,real},g\to q}\hat{\bar{\mathcal{M}}}_{\nu\eta}^{\text{NLO,real},g\to q}\Delta^a(z)\Big],\\
w_{\mu\nu}^{a,q\to g} &= \Delta_g^{\lambda\eta}(z)\,\mathrm{Tr}\Big[\hat{\mathcal{M}}_{\mu\lambda}^{\text{NLO,real},q\to g}\Phi^a(x)\hat{\bar{\mathcal{M}}}_{\nu\eta}^{\text{NLO,real},q\to g}\Big],
\end{aligned} \tag{3.13}$$

where $\Phi_g^{\mu\nu}(x)$ and $\Delta_g^{\mu\nu}(z)$ are the gluon distribution and fragmentation correlators respectively. Next, the phase-space integration over the transverse momentum of the detected hadron can be performed by using symmetry, switching to $d-2$ dimensional spherical coordinates and making use of the delta function. Also, for further manipu-

lation, it is convenient and common to work with scaled variables defined as $w \equiv x_B/x$ and $v \equiv z_h/z$. The $P_{h\perp}$-integrated hadronic tensor then is

$$\begin{aligned}\int \mathrm{d}^{d-2} P_{h\perp} W_{\mu\nu}^{\mathrm{NLO,real}} = \frac{e_a^2 z_h^{1-2\epsilon} x_B}{Q^{2\epsilon} 8\pi^2} S_\epsilon \int_{x_B}^1 \frac{\mathrm{d}w}{w} \int_{z_h}^1 \frac{\mathrm{d}v}{v} \frac{1}{w} \\ \times \left(\frac{v-1}{v}\right)^{-\epsilon} \left(\frac{w-1}{w}\right)^{-\epsilon} w_{\mu\nu}^a \Big|_{\chi_T^2 = (1-\frac{1}{v})(1-\frac{1}{w})}.\end{aligned} \tag{3.14}$$

Evidently the integral is not well-behaved for $w, v \to 1$, since it contains non-integrable functions of w and v. In order to work with well-behaved quantities and extract the singular behavior of the integral we do the following. After performing the Dirac trace, denoting f and D generic PDFs and FFs respectively, we can write the integrated hadronic tensor in the form

$$\int \mathrm{d}^{d-2} P_{h\perp} W_{\mu\nu}^{\mathrm{NLO,real}} = \int_{x_B}^1 \mathrm{d}w \int_{z_h}^1 \mathrm{d}v \; \frac{\hat{\mathcal{W}}_{\mu\nu}(w,v)}{(1-w)^{1+\epsilon}(1-v)^{1+\epsilon}} f(x_B/w) D(z_h/v), \tag{3.15}$$

where $\hat{\mathcal{W}}(w,v)$ is finite in the limit $w, v \to 1$. This re-writing of the integrand allows us to extract the $1/\epsilon$ poles and make them manifest in our expressions. This is because we can now use the useful distribution relation [22]

$$\frac{1}{(1-w)^{1+\epsilon}} = -\frac{1}{\epsilon}\delta(1-w) + \frac{1}{(1-w)_+} - \epsilon \left(\frac{\ln(1-w)}{1-w}\right)_+ + \mathcal{O}(\epsilon^2), \tag{3.16}$$

where the + prescription is defined by [24]

$$\int_{x_B}^1 \mathrm{d}w \, h(w) \left(\frac{g(w)}{1-w}\right)_+ = \int_{x_B}^1 \mathrm{d}w \, \frac{h(w)-h(1)}{1-w} g(w) - h(1) \int_0^{x_B} \mathrm{d}w \frac{g(w)}{1-w}. \tag{3.17}$$

Naturally, these distributional identities are analogous for v as well. This procedure makes the $1/\epsilon$ poles explicit and leads to the well-known cancellation of infrared singularities between real and virtual contributions (commonly referred as infrared safety [15]). We do indeed observe this cancellation of $1/\epsilon^2$ poles in our calculation. However, the partonic cross section typically still exhibits collinear singularities emerging when the parton (coming from the nucleon or fragmenting) becomes collinear with the unobserved parton [11]. The standard procedure is to absorb these collinear poles into $\overline{\mathrm{MS}}$-renormalized parton distribution and fragmentation functions [1, 6]. The corresponding

poles can be removed in the $\overline{\text{MS}}$ scheme by introducing renormalized functions

$$\begin{aligned} f^q_{\text{bare}}(x,\mu) &= f^q_{\text{ren}}(x,\mu) + \frac{\alpha_S}{2\pi}\frac{S_\epsilon}{\epsilon}\left[P_{qq}\otimes f^q_{\text{ren}} + P_{qg}\otimes f^g_{\text{ren}}\right](x,\mu) \\ D^q_{\text{bare}}(z,\mu) &= D^q_{\text{ren}}(z,\mu) + \frac{\alpha_S}{2\pi}\frac{S_\epsilon}{\epsilon}\left[P_{qq}\otimes D^q_{\text{ren}} + P_{gq}\otimes D^g_{\text{ren}}\right](z,\mu) \end{aligned} \tag{3.18}$$

with splitting functions

$$\begin{aligned} P_{qq}(y) &= C_F\left[\frac{1+y^2}{(1-y)_+} + \frac{3}{2}\delta(1-y)\right] \\ P_{qg}(y) &= T_F\left[y^2+(1-y)^2\right] \\ P_{gq}(y) &= C_F\left[\frac{1+(1-y)^2}{y}\right] \end{aligned} \tag{3.19}$$

where the convolution $\otimes$ is a short-hand for

$$(P\otimes f)(x) \equiv \int_x^1 \frac{\mathrm{d}y}{y} P(y) f\left(\frac{x}{y}\right) \tag{3.20}$$

With such splitting functions, inserting the bare distributions into the LO expression for the cross section leads to additional terms that precisely cancel the collinear poles associated with the observed partons in the NLO partonic cross section.
We obtain the following unpolarized NLO result, which is consistent with the literature [8]

$$\begin{aligned} \frac{\mathrm{d}\sigma^{UU}_{\text{LO+NLO}}}{\mathrm{d}x_B\mathrm{d}y\mathrm{d}\phi_l\mathrm{d}z_h} &= \frac{2\alpha^2_{\text{em}}}{yQ^2}\left[\left(1-y+\frac{y^2}{2}\right)F_{UU,T} + (1-y)F_{UU,L}\right] \\ F_{UU,T}(x_B,z_h,Q^2) &= \sum_a e_a^2\Big(f_1^a\circ\mathcal{C}_U^{a\to a}\circ D_1^a + f_1^g\circ\mathcal{C}_U^{g\to a}\circ D_1^a + f_1^a\circ\mathcal{C}_U^{a\to g}\circ D_1^g\Big) \\ F_{UU,L}(x_B,z_h,Q^2) &= \sum_a e_a^2\Big(f_1^a\circ\mathcal{C}_L^{a\to a}\circ D_1^a + f_1^g\circ\mathcal{C}_L^{g\to a}\circ D_1^a + f_1^a\circ\mathcal{C}_L^{a\to g}\circ D_1^g\Big) \end{aligned} \tag{3.21}$$

where we introduced the double convolution $a\circ b\circ c$ defined as

$$f\circ\mathcal{C}\circ D = \int_{x_B}^1\frac{\mathrm{d}w}{w}\int_{z_h}^1\frac{\mathrm{d}v}{v} f\left(\frac{x_B}{w}\right)\mathcal{C}\left(w,v\right)D\left(\frac{z_h}{v}\right) \tag{3.22}$$

The functions $\mathcal{C}_U$ and $\mathcal{C}_L$ are the unpolarized NLO hard-scattering coefficients relative

to the unpolarized structure functions $F_{UU,U}$ and $F_{UU,L}$ respectively [2]. It is very interesting to note that the unpolarized structure function $F_{UU,L}$ is populated at NLO, while it is zero at LO. The coefficients $\mathcal{C}_U$ and $\mathcal{C}_L$ are given by

$$\begin{aligned}
\mathcal{C}_U^{a\to a}(w,v) &= \left[1+\frac{\alpha_S(\mu)}{2\pi}C_F\left(-8-3\ln\frac{\mu^2}{Q^2}\right)\right]\delta(1-w)\delta(1-v)\\
&+\frac{\alpha_S(\mu)}{2\pi}C_F\left[(1+v^2)\left(\frac{\ln(1-v)}{1-v}\right)_+ +1-v+(1+v^2)\frac{\ln v-\ln\frac{\mu^2}{Q^2}}{(1-v)_+}\right]\delta(1-w)\\
&+\frac{\alpha_S(\mu)}{2\pi}C_F\left[(1+w^2)\left(\frac{\ln(1-w)}{1-w}\right)_+ +1-w+(1+w^2)\frac{-\ln w-\ln\frac{\mu^2}{Q^2}}{(1-w)_+}\right]\delta(1-v)\\
&+\frac{\alpha_S(\mu)}{2\pi}C_F\left[\frac{2v^2w^2-2v^2w-2vw^2+4vw+v^2+w^2-2v-2w+2}{(1-w)_+(1-v)_+}\right]\\
\mathcal{C}_U^{g\to a}(w,v) &= \frac{\alpha_S(\mu)}{2\pi}T_F\left[(w^2+(1-w)^2)\left(\ln\frac{1-w}{w}-\ln\frac{\mu^2}{Q^2}\right)+2w(1-w)\right]\delta(1-v)\\
&+\frac{\alpha_S(\mu)}{2\pi}T_F\left[\frac{(w^2+(1-w)^2)(v^2+(1-v)^2)}{v(1-v)_+}\right]\\
\mathcal{C}_U^{a\to g}(w,v) &= \frac{\alpha_S(\mu)}{2\pi}C_F\left[\frac{1+(1-v)^2}{v}\left(\ln\left(v(1-v)\right)-\ln\frac{\mu^2}{Q^2}\right)+v\right]\delta(1-w)\\
&+\frac{\alpha_S(\mu)}{2\pi}C_F\left[\frac{1+v^2+w^2-2vw^2-2v^2w+2v^2w^2}{v(1-w)_+}\right]
\end{aligned} \tag{3.23}$$

and

$$\begin{aligned}
\mathcal{C}_L^{a\to a}(w,v) &= \frac{\alpha_S(\mu)}{2\pi}C_F\left[4vw\right]\\
\mathcal{C}_L^{g\to a}(w,v) &= \frac{\alpha_S(\mu)}{2\pi}T_F\left[8w(1-w)\right]\\
\mathcal{C}_L^{a\to g}(w,v) &= \frac{\alpha_S(\mu)}{2\pi}C_F\left[4w(1-v)\right]
\end{aligned} \tag{3.24}$$

3.2 Transverse nucleon spin

We now turn our attention to the case of transversely-polarized protons. As already shown at LO (REF), the spin-dependent cross section can be obtained within the collinear twist-3 formalism. Here, we will derive the NLO corrections contributing

to the A_{UT} spin asymmetry. Evidently, the complexity of the calculation increases significantly compared to the unpolarized case. In the literature there are very few similar NLO calculations for SIDIS, and they mostly focus on the $P_{h\perp}$-weigthed asymmetries (ADD LIT and couple phrases). This being said, the NLO methodologies presented in the previous section can be directly generalized to this higher-twist case, provided we take into account the additional structures of twist-3 correlators and handle the relative hard parts and transverse partonic momenta with care. Our calculation closely follows, extends and adapts the techniques developed in [21, 9, 13, 17].

3.2.1 Technical aspects

Let us start with the virtual corrections. The NLO diagrams contributing at the twist-3 level are identical to the unpolarized case, when it comes to intrinsic and kinematical contributions (see Fig. 3.1). For those terms, we employ the same methods as in the leading-twist NLO case but with different correlators structures. For dynamical twist-3 though,there are more diagrams that have to be taken into account. The virtual dynamical twist-3 diagrams relevant at NLO are shown in Fig. 3.4. As before, we write the loop momenta in their light-cone decomposition $\mathrm{d}^d r = \mathrm{d}\alpha\, \mathrm{d}^{d-2} r_\perp\, \mathrm{d}\beta$ and perform contour integration over the longitudinal momentum fraction β. Next, the transverse components are integrated out in $d-2$ dimensions. Lastly, the integral over the longitudinal momentum fraction α is performed. Similarly to the unpolarized case, we find that self-energy diagrams for external quark and gluon lines vanish (diagrams a, c, d, e, f, n and o), since they are given by massless integrals. We are therefore left with eight diagrams: the self-energy graph b, the vertex corrections g, h, i, m and the box diagrams j, k and l. As pointed out already, treating gluons in light-cone gauge is advantageous within the twist-3 formalism. In fact, not only we can easily derive a factorization formula at sub-leading twist, but also the gauge invariance of partonic cross sections can be tested throughout the calculation. By writing the polarization sum for gluons as

$$\sum_{\lambda=\pm 1} \epsilon^\mu_\lambda(r)\, \epsilon^{\nu *}_\lambda(r) = -g^{\mu\nu} + \kappa\, \frac{r^\mu m^\nu + r^\nu m^\mu}{r\cdot m}, \tag{3.25}$$

we can easily check if the gauge parameter κ drops out of the final result, as it should, proving the gauge invariance of the cross section. For virtual graphs, we find that

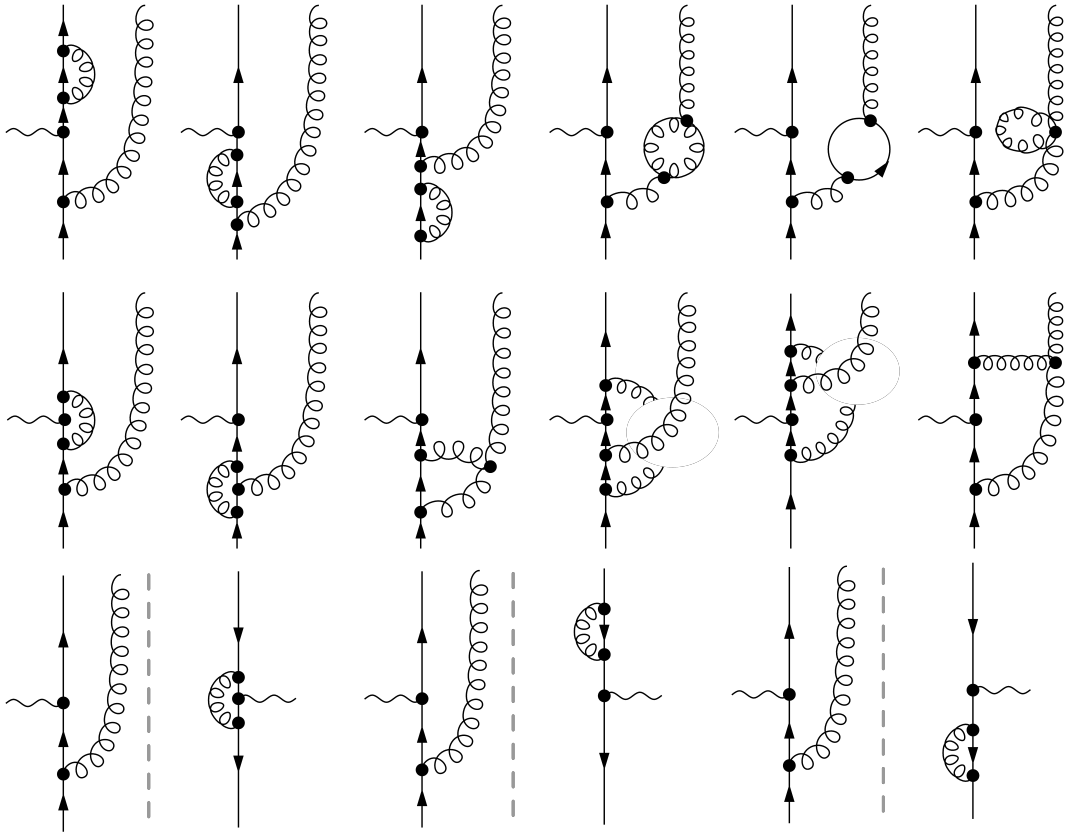

Figure 3.4: Virtual diagrams contributing to the NLO dynamical twist-3 qg fragmentation channel.

gauge invariance is restored only when all the diagrams in Fig. 3.4 are added, since individual diagrams depend on κ. Lastly, we find that classifying the different contributions depending on their color structure helps to organize the calculation in a cleaner way. We therefore separate terms proportional to C_F and N_C and eventually check gauge-invariance and IR-safety separately.

We now move on to the case of real radiation. Similarly to the unpolarized case, at NLO more partonic channels become available. In fact, at NLO not only the qg fragmentation channel contributes, but also $q\bar{q}$ and gg fragmentation channels, in principle. The latter, actually, only contributes if the outgoing hadron is polarized, which is not the case here. Hence, for our observable of interest we only need the qg and $q\bar{q}$ channels.

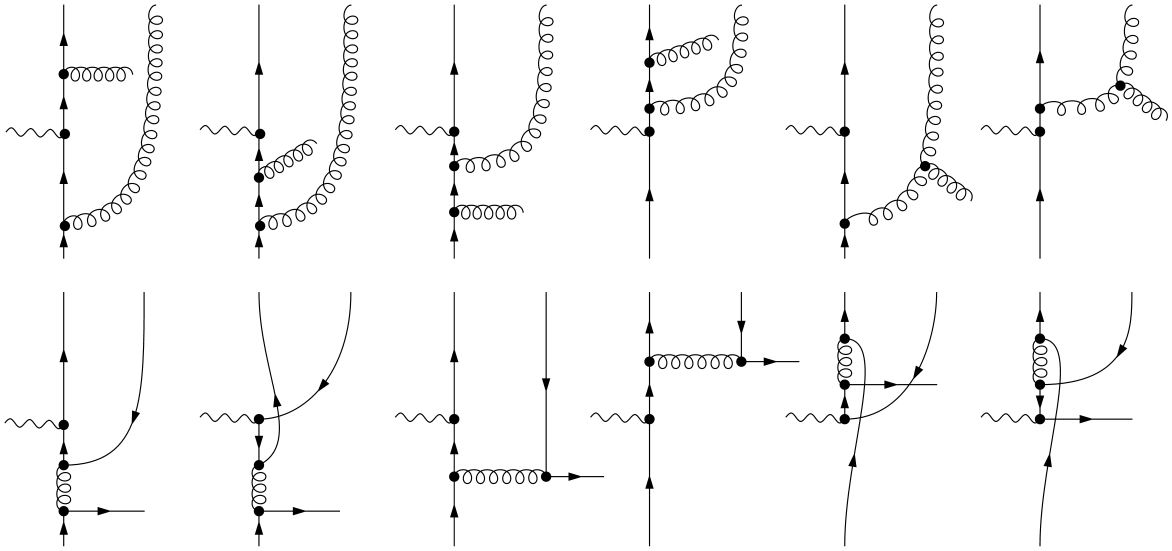

Figure 3.5: Real diagrams contributing to the NLO dynamical twist-3 fragmentation process. (Top row) qg fragmentation channel. Each of these diagrams interferes with the two leading-twist real $q \to q$ NLO corrections in Fig. 3.3. (Bottom row) $q\bar{q}$ fragmentation channel. Each of these diagrams interferes with the two leading-twist real $q \to g$ NLO corrections in Fig. 3.3

Focusing on the qg fragmentation channel, there can only be emission of gluons. Hence, real NLO corrections in the twist-3 case are simply obtained by adding gluon lines to LO twist-3 fragmentation diagrams. Again, for intrinsic and kinematical contributions, the graphs are identical to the leading twist case in the $q \to q$ channel. When it comes to dynamical twist-3, the relevant diagrams are shown in Fig. 3.5. Here, we employ the same phase-space integration techniques used in the unpolarized case. It is important to point out that the hadronic tensor stemming from these diagrams is not gauge invariant. Interestingly, the fact that real NLO corrections at sub-leading twist are κ-dependent has already been observed in the literature [21, 9]. We observe that gauge invariance is restored after combing all twist-3 contributions through EOM and LIR relations, once again proving the importance of these operator identities within this formalism. In the typical leading-twist case, adding virtual and real corrections leads to the well known cancellation of $1/\epsilon^2$ poles. Not surprisingly, we observe this cancellation also at the twist-3 level, after application of EOM and LIR relations.

When it come to the $q\bar{q}$ case, real emission of quarks is taken into account. The

relevant diagrams are shown in Fig. **??**. We observe that the hadronic tensor is κ-gauge invariant and electromagnetic gauge invariant, since it is the only contribution in this channel. It also $1/\epsilon^2$ poles free, in agreement with the fact that there are no virtual corrections to cancel these double poles emerging from the phase space integration. In this sense, the $q\bar{q}$ channel is significantly simpler compared to the qg one and we regard it as a "stand-alone" channel. This is particularly useful when it comes to renormalization, as we will see in the next section. If the IR behaviour of this channel is in agreement with the evolution equations of the relevant fragmentation functions, then we regard it as a strong clue that our calculation is consistent.

Once all the terms are added and combined through the EoMR, we obtain gauge invariant partonic cross sections, free of $1/\epsilon^2$ poles and exhibiting electromagnetic gauge invariance for both channels. We are now left with soft and collinear singularities that can be absorbed, as standard, into renormalized PDFs and FFs. It turns out that the $\overline{\text{MS}}$-renormalization of chiral-odd twist-3 fragmentation functions is significantly more involved compared to the one given by the usual leading-twist DGLAP splitting kernels. The evolution is described by a set of coupled integro-differential equations, mixing different twist-3 contributions, and it has been derived in Ref. [18]. Crucially, we observe that the collinear singularities emerging from our NLO calculation match exactly with these evolution equations, with the appropriate change of conventions between hadronic matrix elements and variables. It is also very relevant to point out that one could wonder whether the EoMR and LIR relations derived at LO would still hold after renormalization at NLO. In Ref. [18] they numerically verified that this is indeed the case, at least for the chiral-odd twist-3 FFs, which is a highly non-trivial result. This means that the twist-3 $\overline{\text{MS}}$-subtraction can be, in principle, performed either *before* or *after* the application of the EoMR.

3.2.2 Results

Chapter 4

Phenomenological and numerical analysis

We saw that factorization holds also at NLO .... bla bla
It is now interesting to numerically explore our analytical formulae to see if and how the NLO corrections affect the theoretical prediction of the spin asymmetry $A_{UT}^{\sin\phi_S}$.

We stress the fact that the quantitative analysis of the $A_{UT}^{\sin\phi_S}$ SSA is quite a recent development in the field of QCD hadron structure and phenomenology. In fact, measurements of the $A_{UT}^{\sin\phi_S}$ asymmetry in SIDIS have become available from the HERMES collaboration only in 2020 [5]. With this set of recent data, the Jefferson Lab Angular Momentum (JAM) collaboration managed to obtain the first ever information about the quark-gluon-quark fragmentation function $\tilde{H}(z)$ within a global QCD analysis [10]. In the same work, transversity has been extracted including lattice QCD data and proper constraints regarding the Soffer bound, giving the smallest uncertainty on the function so far. With these ingredients, we are now in a position to perform some order of magnitude exploratory estimates of the NLO corrections we calculated. We anticipate the fact that our curves cannot be interpreted as real theoretical predictions, since the twist-3 fragmentation functions $\mathrm{Im}\,\hat{H}_{FU}^{qg}(z,\zeta)$ and $\mathrm{Im}\,\hat{H}_{FU}^{\bar{q}q}(z,\zeta)$ are essentially unknown (besides symmetry and few other constraints).

4.1 Transversity and the $\tilde{H}$ fragmentation function

Before dealing with the NLO corrections to the asymmetry, it is useful to visualize the most recent exctractions for both the transversity PDF $h_1^q(x)$ and the quark-gluon-quark fragmentation function $\tilde{H}^q(z)$. As shown in Fig. 4.1, transversity is extracted for u and d quarks. Antiquarks distributions can effectively be ignored since they lead to very small contributions and no overall improvement of the quality of the global fit. However, they will play an important role in the analysis of future data from facilities such as the EIC. Here, we set them to zero for simplicity. More interestingly, the $\tilde{H}(z)$ fragmentation function turns out to behave similarly to the first moment of the Collins FF $H_1^{\perp(1)}(z)$. This is not entirely surprising since the two functions are related to each other via an EoMR (Eq. (1.13)) and they are essentially derived from the same underlying quark-gluon-quark correlator [14]. In [10], they extracted favored $\tilde{H}^{\text{fav}}$ and unfavored $\tilde{H}^{\text{unf}}$ fragmentation functions. These two extractions differ by a sign and describe effects roughly equal in size (with a slightly larger effect for the unfavored channel). By favored hadronization we simply mean the case of a u quark decaying into a positive pion $u\bar{d}$, or a d quark into a negative pion $d\bar{u}$. Explicitly, it is $\tilde{H}^{\text{fav}} = \tilde{H}^{u\to\pi^+} = \tilde{H}^{\bar{d}\to\pi^+} = \tilde{H}^{\bar{u}\to\pi^-} = \tilde{H}^{d\to\pi^-}$. Similarly, the unfavored decay channel refers to a "crossing" between the outgoing quark and the detected hadron, i.e. $\tilde{H}^{\text{unf}} = \tilde{H}^{u\to\pi^-} = \tilde{H}^{\bar{d}\to\pi^-} = \tilde{H}^{\bar{u}\to\pi^+} = \tilde{H}^{d\to\pi^+}$. Very interestingly, unfavored fragmentation seems to be the dominant effect between the two when it comes to the $A_{UT}^{\sin\phi_S}$ asymmetry, as clearly showcased later. Lastly, we mention that these extractions are performed at the scale $Q^2 = 4\,\text{GeV}^2$. For transversity, being a leading twist distribution, a DGLAP scale evolution is implicitly implemented in our numerical analysis through the LHAPDF interface [**<empty citation>**]. On the other hand, the evolution for $\tilde{H}(z)$ is significantly more involved, as already pointed out in Chap. 3. The evolution equations are known [18] but, unfortunately, there is still no available code that calculates this scale evolution for sub-leading twist fragmentation functions. Ignoring evolution for twist-3 FFs is is not a tremendous problem at LO, but it starts to be a crude approximation when the calculation is pushed at NLO accuracy in α_S. This being said, we still believe that an exploratory estimate can be presented, as a proof of principle that NLO corrections to twist-3 distributions play an integral part in the phenomenology of SSAs.

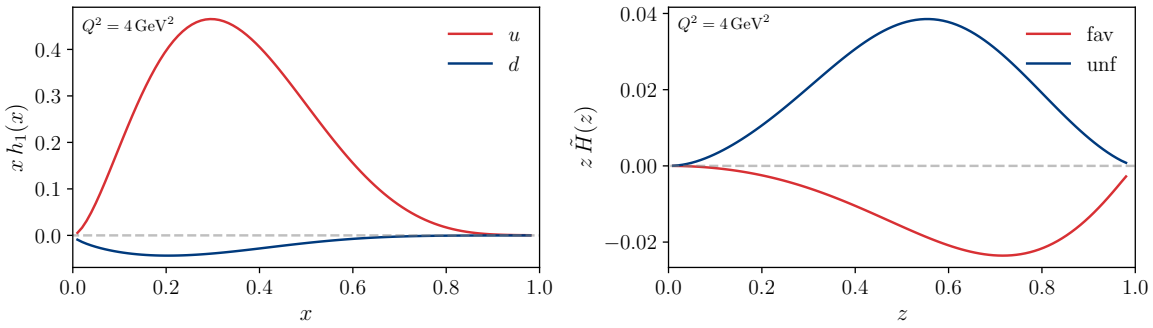

Figure 4.1: Non-perturbative functions entering the numerator of the $A_{UT}^{\sin\phi_S}$ spin asymmetry. Transversity PDF $h_1(x)$ (left) and QGQ fragmentation function $\tilde{H}(z)$ (right). The parametrizations are taken from the JAM22 analysis [10].

4.2 The $A_{UT}^{\sin\phi_S}$ spin asymmetry

In order to compare the $A_{UT}^{\sin\phi_S}$ theoretical prediction against 3D-binned HERMES data we need to point several important aspects. The first being the fact that we are interested in an observable which is integrated over $P_{h\perp}$, the transverse momentum of the detected hadron. As seen in Chap. 2, the only term in the structure function $F_{UT}^{\sin\phi_S}$ that survives the integration over the transverse momentum is the one coupling the transversity PDF $h_1(x)$ and the FF $\tilde{H}(z)$. Hence, in order to be directly sensitive to $\tilde{H}(z)$ in an experiment, one should in principle integrate over all possible transverse hadronic momenta. This however could not be done experimentally at HERMES. For this precise reason, we make the assumption that taking only the x_B and z_h projections of the $A_{UT}^{\sin\phi_S}$ HERMES data is a reasonable approximation [10]. In practice, we set all the kinematical variables (except the projected one) to their experimental average, easily found in Table 10 Ref. [5]. Another important point concerns the (de)polarization factors entering the spin asymmetry. Recalling Chap. 2, the asymmetry can be written as CHECK

$$A_{UT}^{\sin\phi_S} = \sqrt{2\varepsilon(1+\varepsilon)}\frac{\int d^2P_{h\perp}\, F_{UT}^{\sin\phi_S}(x_B, z_h, P_{h\perp}, Q^2)}{\int d^2P_{h\perp}\, F_{UU}(x_B, z_h, P_{h\perp}, Q^2)}, \tag{4.1}$$

where the $\sqrt{2\varepsilon(1+\varepsilon)}$ term is the depolarization factor for this polarization case. Conveniently, HERMES asymmetry data is presented both including or excluding this factor. For simplicity, we use the scaled data in which the polarization factor is divided away.

Hence, the observable we are going to numerically study is simply given by the ratio of the ($P_{h\perp}$-integrated) structure functions, i.e.

$$\left(A_{UT}^{\sin\phi_S}\right)_{\text{exp}} = \frac{\int d^2P_{h\perp}\, F_{UT}^{\sin\phi_S}(x_B, z_h, P_{h\perp}, Q^2)}{\int d^2P_{h\perp}\, F_{UU}(x_B, z_h, P_{h\perp}, Q^2)}. \tag{4.2}$$

We stress the fact that the unpolarized structure function at LO is simply given by $F_{UU} = F_{UU,T}$, meaning only transverse photons contribute. However, at NLO more partonic channels become available and therefore the asymmetry denominator becomes $F_{UU} = F_{UU,T} + \varepsilon F_{UU,L}$.

The asymmetry at leading-order in α_S is shown in Fig. 4.2. The leading-order curves are obtained by employing the YYY PDF set REF and ZZZ FF set at LO accuracy, and setting the unprojected kinematical variables to their experimental average, as mentioned before. These curves are analogous to the ones presented in the global analysis in Ref. [10]. The fact that the LO projections describe reasonably well HERMES data should not be surprising, since this precise data set has been crucial for the extraction of the $\tilde{H}(z)$ fragmentation function. The HERMES collaboration claims the measurement of the $A_{UT}^{\sin\phi_S}$ asymmetry as one of the most striking results of their analysis. This is because this specific observable has by far the largest twist-3 signal among all sub-leading twist effects. The observation is particularly true for π^- production, where the asymmetry is significantly different from zero, of the order of -2% at least in the studied kinemtical region. Another unexpected and surprising feature revealed by this measurement is the strong kinematic dependence. In fact, the magnitude of the asymmetry significantly rises with increasing x_B and z_h, reaching values up to 10% at the edge of the z_h phase space.

In order to perform a NLO exploratory study, we need one last ingredient: input fragmentation functions $\text{Im}\,\hat{H}_{FU}^{qg}(z,\zeta)$ and $\text{Im}\,\hat{H}_{FU}^{\bar{q}q}(z,\zeta)$ for all flavors q. Since these functions are currently unknown, a real prediction is clearly not possible. We can, though, build some models respecting the currently known constraints and plot the resulting curves for different choices of parameters. A typical parametrization for collinear PDFs and FFs is given by the formula [10]

$$P^q(x) \equiv \frac{N^q\, x^{a_q}(1-x)^{b_q}\left(1+\gamma^q x^{\tilde{a}_q}(1-x)^{\tilde{b}_q}\right)}{\mathbb{B}(a_q+2, b_q+1) + \gamma^q \mathbb{B}(a_q+\tilde{a}_q+2, b_q+\tilde{b}_q+1)}, \tag{4.3}$$

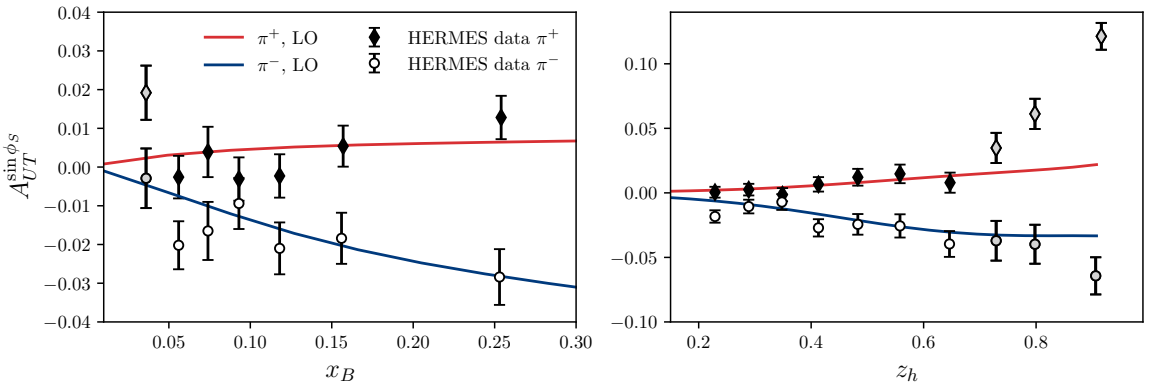

Figure 4.2: Projections along x_B and z_h of the (scaled) single spin asymmetry $A_{UT}^{\sin\phi_S}$ at leading-order in α_S. As mentioned in [10], grey data points in the x_B projection are excluded in the fitting procedure of $\tilde{H}(z)$ since $Q^2 \sim 1\,\mathrm{GeV}^2$ for those data points. Similarly, in the z_h projection the grey data points are not included in other projections and neither are included in the fitting of $\tilde{H}(z)$, since the standard semi-inclusive region corersponds to the kinemtical cut $0.2 < z_h < 0.7$ [5].

where $\mathbb{B}(a,b)$ is the Euler beta function. Based on this, we construct some simple models for the fragmentation functions of interest. For simplicity, we set to zero the $\gamma, \tilde{a}, \tilde{b}$ parameters, only allowing others to vary. We set

$$\begin{aligned} \operatorname{Im} \hat{H}_{FU}^{qg}(z,\zeta) &= \frac{\tilde{H}(z)}{2z} \frac{\zeta^{a_q}(1-\zeta)^{b_q}}{\mathbb{B}(1+a_q, b_q)}, \\ \operatorname{Im} \hat{H}_{FU}^{\bar{q}q}(z,\zeta) &= \frac{\tilde{H}(z)}{2z} \frac{N^q\,\zeta^{c_q}(1-\zeta)^{c_q}}{\mathbb{B}(1+c_q, 1+c_q)}. \end{aligned} \tag{4.4}$$

It is important to note that in the qg case, our model is guaranteed to satisfy the EoM relation $\tilde{H}(z)/2z = \int \mathrm{d}\zeta \operatorname{Im} \hat{H}_{FU}^{qg}(z,\zeta)/(1-\zeta)$ by construction. This is the case also for the boundary conditions presented in Chap. 1, such as $\operatorname{Im} \hat{H}_{FU}^{qg}(z,0) = \operatorname{Im} \hat{H}_{FU}^{qg}(z,1) = \partial_\zeta \operatorname{Im} \hat{H}_{FU}^{qg}(z,\zeta)|_{\zeta\to 0} = \partial_\zeta \operatorname{Im} \hat{H}_{FU}^{qg}(z,\zeta)|_{\zeta\to 1} = 0$, provided we choose appropriate model parameters. When it comes to the $\bar{q}q$ correlator, it is completely unconstrained. We choose however to model it such that the z-dependence precisely matches the quark-gluon-quark FF $\tilde{H}(z)$. After all, these twist-3 objects are all interconnected to one another, and we regard it as a reasonable and very simple assumption. We would expect the $\bar{q}q$ correlator to be symmetric(??) under the exchange of quarks and antiquarks, hence why we set the exponents of ζ and $(1-\zeta)$ to be equal for a given

q. In order to compare LO and NLO x and z projections, we generate various so called scenarios. We define a scenario as one specific set of model parameters including both fragmentation functions. Meaning, the k-th scenario is described by the set $S_k = \{a_u, a_{\bar{u}}, a_d, a_{\bar{d}}, b_u, b_{\bar{u}}, \dots\}$. To generate these scenarios, we sample each parameter from a uniform distribution. EXPLAIN HERE UNIFORM SAMPLING AND LIMITS USED, IF NECESSARY.

The results of our exploratory NLO numerical analysis are presented in Fig. 4.3. Here, the projections along x_B and z_h of the spin asymmetry are shown, for both π^+ and π^- production. The NLO curves, corresponding to ZZZ different scenarios, exhibit quite different behavior. This is a strong indication of the fact that the NLO corrections to the asymmetry are quite sensitive to the choice of parameters used to describe the QGQ correlators, as well as their model parametrization overall. In principle, one could perform a fit to the experimental data to constrain the QGQ correlators. This is beyond the scope of this work and it may be subject of future investigations.

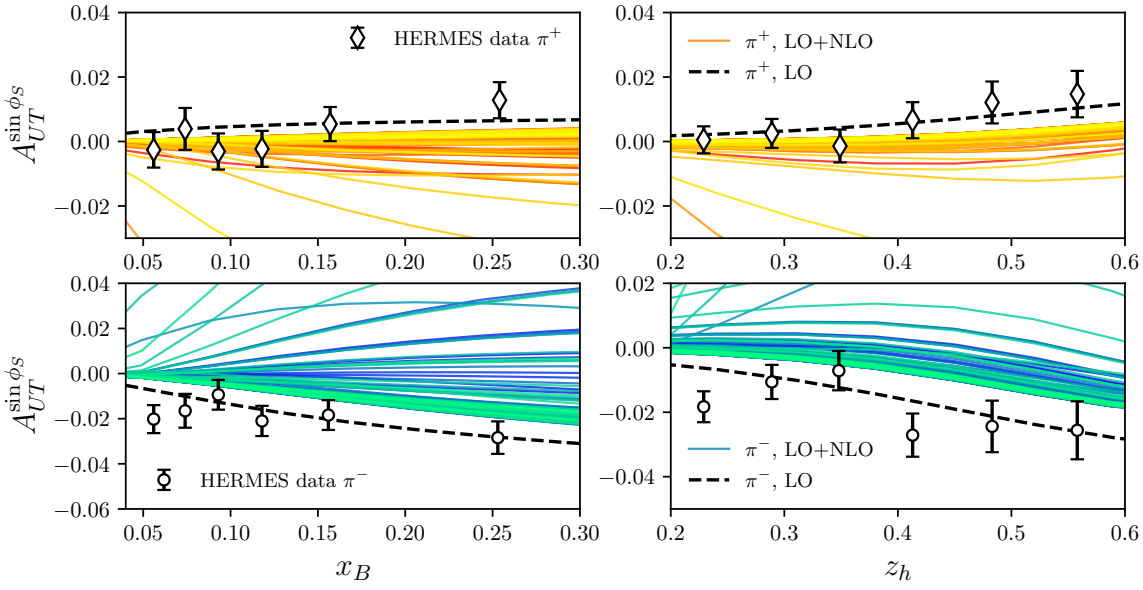

Figure 4.3: Projections along x_B and z_h of the (scaled) single spin asymmetry $A_{UT}^{\sin\phi_S}$. The colored curves correspond to different scenarios S_j, i.e. different models for the twist-3 FFs $\mathrm{Im}\,\hat{H}_{FU}^{qg}(z,\zeta)$ and $\mathrm{Im}\,\hat{H}_{FU}^{\bar{q}q}(z,\zeta)$.

The are essentially two important outcomes of this exploratory NLO study. First,

one sees that the NLO corrections to the numerator of the SSA can be large, and not at all negligible. In numerous scenarios we even witness NLO corrections so large that the asymmetry changes sign. This fact alone should be enough to remark the importance of NLO corrections to spin-dependent observables in QCD. We also note the fact that NLO corrections to the numerator of SSAs can be large has been numerically tested in a very similar manner also for single inclusive hadron production $ep \to hX$ [21]. Secondly, the fact that the NLO single-spin asymmetry shows great sensitivity to the set of employed twist-3 matrix elements motivates even more the importance of future precision colliders such as the EIC. In fact, future accurate data collected at larger center-of-mass energies will deepen our understanding of sub-leading twist distribution and fragmentation effects, shedding light on detailed hadron structure and the hadronization mechanism.

Conclusions

Lorem ipsum dolor sit amet, consectetuer adipiscing elit. Ut purus elit, vestibulum ut, placerat ac, adipiscing vitae, felis. Curabitur dictum gravida mauris. Nam arcu libero, nonummy eget, consectetuer id, vulputate a, magna. Donec vehicula augue eu neque. Pellentesque habitant morbi tristique senectus et netus et malesuada fames ac turpis egestas. Mauris ut leo. Cras viverra metus rhoncus sem. Nulla et lectus vestibulum urna fringilla ultrices. Phasellus eu tellus sit amet tortor gravida placerat. Integer sapien est, iaculis in, pretium quis, viverra ac, nunc. Praesent eget sem vel leo ultrices bibendum. Aenean faucibus. Morbi dolor nulla, malesuada eu, pulvinar at, mollis ac, nulla. Curabitur auctor semper nulla. Donec varius orci eget risus. Duis nibh mi, congue eu, accumsan eleifend, sagittis quis, diam. Duis eget orci sit amet orci dignissim rutrum.

Nam dui ligula, fringilla a, euismod sodales, sollicitudin vel, wisi. Morbi auctor lorem non justo. Nam lacus libero, pretium at, lobortis vitae, ultricies et, tellus. Donec aliquet, tortor sed accumsan bibendum, erat ligula aliquet magna, vitae ornare odio metus a mi. Morbi ac orci et nisl hendrerit mollis. Suspendisse ut massa. Cras nec ante. Pellentesque a nulla. Cum sociis natoque penatibus et magnis dis parturient montes, nascetur ridiculus mus. Aliquam tincidunt urna. Nulla ullamcorper vestibulum turpis. Pellentesque cursus luctus mauris.

Nulla malesuada porttitor diam. Donec felis erat, congue non, volutpat at, tincidunt tristique, libero. Vivamus viverra fermentum felis. Donec nonummy pellentesque ante. Phasellus adipiscing semper elit. Proin fermentum massa ac quam. Sed diam turpis, molestie vitae, placerat a, molestie nec, leo. Maecenas lacinia. Nam ipsum ligula, eleifend at, accumsan nec, suscipit a, ipsum. Morbi blandit ligula feugiat magna. Nunc eleifend consequat lorem. Sed lacinia nulla vitae enim. Pellentesque tincidunt purus vel

magna. Integer non enim. Praesent euismod nunc eu purus. Donec bibendum quam in tellus. Nullam cursus pulvinar lectus. Donec et mi. Nam vulputate metus eu enim. Vestibulum pellentesque felis eu massa.

Quisque ullamcorper placerat ipsum. Cras nibh. Morbi vel justo vitae lacus tincidunt ultrices. Lorem ipsum dolor sit amet, consectetuer adipiscing elit. In hac habitasse platea dictumst. Integer tempus convallis augue. Etiam facilisis. Nunc elementum fermentum wisi. Aenean placerat. Ut imperdiet, enim sed gravida sollicitudin, felis odio placerat quam, ac pulvinar elit purus eget enim. Nunc vitae tortor. Proin tempus nibh sit amet nisl. Vivamus quis tortor vitae risus porta vehicula.

Bibliography

[1] G. Altarelli, R.K. Ellis, and G. Martinelli. "Large perturbative corrections to the Drell-Yan process in QCD". en. In: *Nuclear Physics B* 157.3 (Oct. 1979), pp. 461–497. ISSN: 05503213. DOI: 10.1016/0550-3213(79)90116-0. URL: https://linkinghub.elsevier.com/retrieve/pii/0550321379901160 (visited on 02/13/2025).

[2] Alessandro Bacchetta et al. "Semi-inclusive deep inelastic scattering at small transverse momentum". en. In: *Journal of High Energy Physics* 2007.02 (Feb. 2007). arXiv:hep-ph/0611265, pp. 093–093. ISSN: 1029-8479. DOI: 10.1088/1126-6708/2007/02/093. URL: http://arxiv.org/abs/hep-ph/0611265 (visited on 02/07/2025).

[3] Alessandro Bacchetta et al. "Single-spin asymmetries: the Trento conventions". en. In: *Physical Review D* 70.11 (Dec. 2004). arXiv:hep-ph/0410050, p. 117504. ISSN: 1550-7998, 1550-2368. DOI: 10.1103/PhysRevD.70.117504. URL: http://arxiv.org/abs/hep-ph/0410050 (visited on 02/06/2025).

[4] Daniel Boer, P. J. Mulders, and F. Pijlman. "Universality of T-odd effects in single spin and azimuthal asymmetries". en. In: *Nuclear Physics B* 667.1-2 (Sept. 2003). arXiv:hep-ph/0303034, pp. 201–241. ISSN: 05503213. DOI: 10.1016/S0550-3213(03)00527-3. URL: http://arxiv.org/abs/hep-ph/0303034 (visited on 02/06/2025).

[5] HERMES Collaboration et al. *Azimuthal single- and double-spin asymmetries in semi-inclusive deep-inelastic lepton scattering by transversely polarized protons.* 2020. arXiv: 2007.07755 [hep-ex]. URL: https://arxiv.org/abs/2007.07755.

[6] John Collins. *Foundations of Perturbative QCD.* Cambridge Monographs on Particle Physics, Nuclear Physics and Cosmology. Cambridge University Press, 2011.

[7] P. Dennery and A. Krzywicki. *Mathematics for Physicists*. Dover Books on Physics. Dover Publications, 2012. ISBN: 9780486157122. URL: https://books.google.de/books?id=ogHCAgAAQBAJ.

[8] D. de Florian, M. Stratmann, and W. Vogelsang. "QCD analysis of unpolarized and polarized Λ-baryon production in leading and next-to-leading order". In: *Physical Review D* 57.9 (May 1998), 5811–5824. ISSN: 1089-4918. DOI: 10.1103/physrevd.57.5811. URL: http://dx.doi.org/10.1103/PhysRevD.57.5811.

[9] Leonard Gamberg et al. "Polarized hyperon production in single-inclusive electron-positron annihilation at next-to-leading order". In: *Journal of High Energy Physics* 2019.1 (Jan. 2019). ISSN: 1029-8479. DOI: 10.1007/jhep01(2019)111. URL: http://dx.doi.org/10.1007/JHEP01(2019)111.

[10] Leonard Gamberg et al. "Updated QCD global analysis of single transverse-spin asymmetries: Extracting H˜, and the role of the Soffer bound and lattice QCD". In: *Phys. Rev. D* 106.3 (2022), p. 034014. DOI: 10.1103/PhysRevD.106.034014. arXiv: 2205.00999 [hep-ph].

[11] Patriz Hinderer, Marc Schlegel, and Werner Vogelsang. "Single-Inclusive Production of Hadrons and Jets in Lepton-Nucleon Scattering at NLO". en. In: *Physical Review D* 92.1 (July 2015). arXiv:1505.06415 [hep-ph], p. 014001. ISSN: 1550-7998, 1550-2368. DOI: 10.1103/PhysRevD.92.014001. URL: http://arxiv.org/abs/1505.06415 (visited on 02/06/2025).

[12] T. Huber and D. Maître. "HypExp, a Mathematica package for expanding hypergeometric functions around integer-valued parameters". In: *Computer Physics Communications* 175.2 (July 2006), 122–144. ISSN: 0010-4655. DOI: 10.1016/j.cpc.2006.01.007. URL: http://dx.doi.org/10.1016/j.cpc.2006.01.007.

[13] Koichi Kanazawa and Yuji Koike. "Contribution of the twist-3 fragmentation function to the single transverse-spin asymmetry in semi-inclusive deep inelastic scattering". en. In: *Physical Review D* 88.7 (Oct. 2013), p. 074022. ISSN: 1550-7998, 1550-2368. DOI: 10.1103/PhysRevD.88.074022. URL: https://link.aps.org/doi/10.1103/PhysRevD.88.074022 (visited on 02/06/2025).

[14] Koichi Kanazawa et al. "Operator Constraints for Twist-3 Functions and Lorentz Invariance Properties of Twist-3 Observables". en. In: *Physical Review D* 93.5 (Mar. 2016). arXiv:1512.07233 [hep-ph], p. 054024. ISSN: 2470-0010, 2470-0029. DOI: 10.1103/PhysRevD.93.054024. URL: http://arxiv.org/abs/1512.07233 (visited on 02/07/2025).

[15] Toichiro Kinoshita. "Mass Singularities of Feynman Amplitudes". In: *Journal of Mathematical Physics* 3.4 (July 1962). _eprint: https://pubs.aip.org/aip/jmp/article-pdf/3/4/650/19167464/650_1_online.pdf, pp. 650–677. ISSN: 0022-2488. DOI: 10.1063/1.1724268. URL: https://doi.org/10.1063/1.1724268.

[16] Yuji Koike, Junji Nagashima, and Werner Vogelsang. "Resummation for polarized semi-inclusive deep-inelastic scattering at small transverse momentum". In: *Nuclear Physics B* 744.1–2 (June 2006), 59–79. ISSN: 0550-3213. DOI: 10.1016/j.nuclphysb.2006.03.009. URL: http://dx.doi.org/10.1016/j.nuclphysb.2006.03.009.

[17] Yuji Koike et al. "Transverse Polarization of Hyperons Produced in Semi-Inclusive Deep Inelastic Scattering". en. In: *Physical Review D* 105.5 (Mar. 2022). arXiv:2202.00338 [hep-ph], p. 056021. ISSN: 2470-0010, 2470-0029. DOI: 10.1103/PhysRevD.105.056021. URL: http://arxiv.org/abs/2202.00338 (visited on 02/06/2025).

[18] J.P. Ma and G.P. Zhang. "Evolution of chirality-odd twist-3 fragmentation functions". In: *Physics Letters B* 772 (Sept. 2017), 559–566. ISSN: 0370-2693. DOI: 10.1016/j.physletb.2017.07.025. URL: http://dx.doi.org/10.1016/j.physletb.2017.07.025.

[19] Ruibin Meng, Fredrick I. Olness, and Davison E. Soper. "Semi-inclusive deeply inelastic scattering at electron-proton colliders". en. In: *Nuclear Physics B* 371.1-2 (Mar. 1992), pp. 79–110. ISSN: 05503213. DOI: 10.1016/0550-3213(92)90230-9. URL: https://linkinghub.elsevier.com/retrieve/pii/0550321392902309 (visited on 02/06/2025).

[20] P. J. Mulders and R. D. Tangerman. "The complete tree-level result up to order $1/Q$ for polarized deep-inelastic leptoproduction". en. In: *Nuclear Physics B* 461.1-2 (Feb. 1996). arXiv:hep-ph/9510301, pp. 197–237. ISSN: 05503213. DOI: 10.1016/0550-3213(95)00632-X. URL: http://arxiv.org/abs/hep-ph/9510301 (visited on 02/06/2025).

[21] Daniel Rein et al. *NLO corrections and factorization for transverse single-spin asymmetries*. 2025. arXiv: 2503.16097 [hep-ph]. URL: https://arxiv.org/abs/2503.16097.

[22] Matthew D. Schwartz. *Quantum Field Theory and the Standard Model*. Cambridge University Press, Mar. 2014.

[23] A. N. Sissakian, O. Yu. Shevchenko, and O. N. Ivanov. "NLO QCD procedure of the semi-inclusive deep inelastic scattering data analysis with respect to the light quark polarized sea". In: *Physical Review D* 70.7 (Oct. 2004). ISSN: 1550-2368. DOI: 10.1103/physrevd.70.074032. URL: http://dx.doi.org/10.1103/PhysRevD.70.074032.

[24] George Sterman et al. "Handbook of perturbative QCD". In: *Rev. Mod. Phys.* 67 (1 Jan. 1995), pp. 157–248. DOI: 10.1103/RevModPhys.67.157. URL: https://link.aps.org/doi/10.1103/RevModPhys.67.157.

[25] Steven Weinberg. *The Quantum Theory of Fields*. Cambridge University Press, 1995.